

Article

Direct Tilt Controller Design with Disturbance Compensation and Implementation for a Narrow Tilting Electric Vehicle

Mustafa Karamuk ^{1,*} and Orhan Behic Alankus ² ¹ Ford Otosan R&D Center, 34885 Istanbul, Turkey² Department of Mechanical Engineering, Faculty of Engineering and Natural Sciences, Istanbul Okan University, Tuzla Campus, 34959 Istanbul, Turkey; orhan.alankus@okan.edu.tr

* Correspondence: mkaramuk@ford.com.tr; Tel.: +90-216-6649128

Abstract: Three-wheeled electric city vehicles are becoming popular because they have lower cost and enable motorcycle driving feeling with electric powertrain performance. These vehicles need a driver assistant system, also known as an active tilting stability controller, to provide a safe cornering manoeuvre. Active tilt control methods are direct tilt control (DTC), steering tilt control (STC) and a combination of these methods. In this study, DTC system design with a servo motor actuator with simulation and experimental results are presented. State feedback control with pole placement design has been improved with disturbance compensation control. This novel controller structure enhances the response of DTC and enables a faster-tilting response. Simulation results are given up to 10 m/s speed. Experimental results of the developed method are given up to 3.05 m/s (11 km/h) speed on a three-wheeled electric vehicle. The speed control loop of the servo motor drive unit (SMDU) stabilizes the DTC system. In the state of the art, a proportional derivative controller is commonly used as a tilt controller. By including the speed control loop of SMDU in the tilt control system, the use of the derivative term can be eliminated. The stability effect of the speed control loop is shown by MATLAB analysis, simulations in Simulink and experimental step response test as well.

Keywords: three-wheeled electric vehicles; vehicle dynamics; direct tilt control; state feedback control; disturbance compensation control; servo motor; motor drive unit



Citation: Karamuk, M.; Alankus, O.B. Direct Tilt Controller Design with Disturbance Compensation and Implementation for a Narrow Tilting Electric Vehicle. *Energies* **2023**, *16*, 5724. <https://doi.org/10.3390/en16155724>

Academic Editor: Alberto Reatti

Received: 25 May 2023

Revised: 23 July 2023

Accepted: 24 July 2023

Published: 31 July 2023



Copyright: © 2023 by the authors. Licensee MDPI, Basel, Switzerland. This article is an open access article distributed under the terms and conditions of the Creative Commons Attribution (CC BY) license (<https://creativecommons.org/licenses/by/4.0/>).

1. Introduction

Three-wheeled light electric vehicles are becoming popular in recent years as cost-effective solutions to traffic congestion and reduction of harmful emissions in big cities. Leading automotive companies such as Ford, Toyota, GM, Mercedes-Benz, and Brink Dynamics developed 3- and 4-wheeled light electric vehicles [1–4], also known as narrow tilting vehicles (NTV).

A three-wheeled vehicle is an unstable system during cornering. Stabilization should be realized by the driver's skills or an active stability controller.

The report in [5] describes the detailed statistics and causes of motorcycle accidents. Active tilting stability controller (ATSC), also known as leaning support, is a driving assistance system that prevents the rollover of NTV by tilting the vehicle automatically. ATSC can prevent accidents during cornering for drivers who do not have motorcycle driving skills.

Regarding the ATSC systems, there are mainly direct tilt control (DTC), steering tilt control (STC) and a combination of both methods (DTC-STC). These methods were studied in detail in [1–4,6–17]. DTC and STC methods have limitations related to vehicle longitudinal speed and actuator sizing. Concept and commercialized NTVs were presented in [1–4]. There are commercially available NTVs equipped with DTC or other ATSC systems [1–4].

DTC enables straightforward controller design. On the other hand, the DTC method requires higher actuator torque, whereas STC enables reduction of actuator torque [1–4,6–17].

Therefore, application of DTC is limited to low-speed and typically up to 10 km/h. The speed limit is dependent on the design of the vehicle and the DTC system as well.

Combination of DTC-STC method was developed as a remedy to speed-dependent performance problems of DTC and STC. DTC-STC combination can utilize the benefits of both methods. But this combined method also has two critical problems: (1) two different actuators for DTC and STC are required, and therefore system cost is increased, and extra space is needed in NTV. (2) Transition between DTC and STC requires a smooth transition, and the control mode changeover problem needs to be solved. Therefore, researchers in [10] proposed STC at high speeds and tilt brake at low speeds to keep the NTV upstand.

1.1. Brief Review of the Recent Studies

Past research and studies have established theoretical background, simulation, and experimental data on tilt control technology, as summarized in [18].

This review includes recent studies on ATCS, including four-wheeled automobiles.

In [4], tilting methods were investigated using a multibody model of a reference NTV. Regarding the control methods, optimal control, gain-scheduling linear quadratic control (LQR), feedback linearization and model predictive control methods were studied, and the last three methods were compared. The studies were carried out on simulation.

ATSC applied for an automobile can improve handling stability and ride comfort and prevents rollover during cornering [19]. An automobile active tilt control based on active suspension was studied with the sliding mode control method in [19]. Passive suspension and active suspension with sliding mode control were presented and compared in simulation to show the effectiveness of the proposed control method for the given simulation cases. In [20,21], rollover index-based tilt control was proposed to determine the desired tilting angle. The actuator is activated based on the rollover index threshold conditions. It is stated that the proposed control method provides energy saving for the actuator and reduction of the control effort. Simulation results in CarSim were given. In [21], a high-level controller was also developed to combine the lateral and longitudinal vehicle dynamics. In [22], the integration of ATCS and full-wheel steering controller for a four-wheel automobile was studied. It was stated that combining the two controllers improved the ride comfort, maneuverability, safety, and the vehicle's lateral control performance. The controllers were designed using the optimal control method, and simulation results were presented. In [23], curve tilting functionality using active suspensions was studied for a four-wheeled vehicle. A non-linear model predictive control method was applied. The controller in [23] was implemented on the dSPACE MicroAutoBox II hardware-in-the-loop (HIL) system. HIL results were presented in urban, rural and highway driving conditions. In [24], the tilting feedforward synchronous control method was proposed. The yaw motion of the NTV was predicted. Based on the predicted yaw rate, tilting feedforward synchronous control method was proposed. The recurrent neural network was used for the prediction of the yaw rate. The proposed method was applied to an experimental NTV. In [25], a robust controller was designed for tilt control of a four-wheel NTV. The tilting control method is the DTC method based on steering angle. A nonlinear vehicle dynamics model of an NTV was developed. Simulation results were given for maneuvers at various longitudinal speeds.

1.2. System Level Parameters Effecting on Tilt Control System Development

The following design and development steps should be considered for any type of ATSC.

1. Selection of tilt control method (DTC, STC, or DTC-STC combination)
2. Selection of the tilt controller type
3. Selection of the actuator type
4. Conceptual study and simulation
5. Software and hardware implementation
6. Integration into the target NTV

7. Experimental tests

When selecting the controller type and control configuration, the cost of the required hardware and microcontroller should be one of the decision factors because NTV should be designed at a lower cost than a passenger car. In the case of advanced types of control methods, such as model predictive control and deep learning control, which require high processor power and memory, the cost of the controller hardware will increase. Total system cost is a critical design factor for prototype development and commercialization.

Another aspect of the selected control method is the required CPU rate, communication speed between the components and number of sensors. Therefore, control configuration affects the total power consumption [26,27]. The same problem exists in autonomous vehicles. On-board computers and sensors increase the power and energy consumption in autonomous vehicles studied in [28]. The same problems should be considered for the tilt control system and its subcomponents. Therefore, the tilt control method, the energy consumption of the sensors, and the controller hardware affect the total energy consumption of the NTV. Despite of increasing trend in electromobility, the use of servo motor as tilt actuators has not been studied in detail in the state of the art. Especially energy consumption of ATSC with a servo motor has not been analyzed experimentally. In that sense, this study also emphasizes the importance of electrification for ATSC. So far, the academic literature on tilt controller design did not study the importance of actuators' efficiency and efficient operating points. This objective can be best achieved by the servo motor actuator system with proper gearbox sizing. Table 1 summarizes essential design-level parameters for tilt control system development. In case of practical application, all of these parameters should be evaluated. In logistic applications, the development of ATSC for motorcycles and NTVs should be realized by low-cost components and low-cost design because of the cost sensitivity in this market. Besides the total cost, vehicles in the logistic market should be operational on dry or wet roads and in hot or cold weather. ATSC and subcomponents should fulfil these requirements.

Table 1. Parameters for Development Process of Tilt Control.

Development Parameters	Vehicle Level Effects	Effect on Tilt Controller Type
Control configuration	Required space	System complexity level
Target market	Target cost for system development	Target cost for tilt controller hardware
Climate	Actuator * torque de-rating risk	Constraint controllers should consider climate effects.
Drive cycle effect	Power sizing, energy management and energy consumption	Required dynamic response
Vehicle configuration (Tadpole, delta, or four wheel NTV)	Personal use or logistic application	The total mass, yaw inertia, tilting inertia, vehicle dynamic response

* for hydraulic and servo motor actuators.

The following design issues are also listed in connection with Table 1.

- Actuator level efficiency: In the state of the art, the design target is typically set such that the perceived acceleration and tilting torque should be zero at a steady-state condition to reduce energy consumption. However, depending on the drive cycle and tilting maneuver, a steady-state condition may not always occur. It is also essential to maintain the efficient operation of the actuator during the transient maneuvers.
- Geometrical integration of ATSC components: NTV has quite a restricted space. Therefore, the selected control method should ensure that the required sensor, actuator system, power supply and other control modules can be mounted to the available space in the target vehicle.
- Real-life drive cycles and tests at real maneuvers at target speeds: ATSCs need a lot of real-life application case studies and feedback from applications to become a mature

technology. To realize this, low-cost solutions are required. To this end, this study aims to contribute to the current state of the art in terms of application case study, simplification of design concepts, and reduction of the number of the required sensors with the proposed control configuration.

Based on real-life observations of motorcycle drivers, it can be concluded that most drivers tilt the NTV even at very low speeds, such as the 5 km/h speed range. Vehicle speed can vary slightly during cornering. They can suddenly stop and then start driving while tilting. Therefore, ideal driving conditions and perfectly coordinated turns at steady-state conditions cannot always occur in real life. DTC is always needed in city traffic.

1.3. Advantages of Servo Motor Actuators

The servo motor in this study refers to a permanent magnet synchronous motor with sinusoidal operation mode. A comparison of hydraulic and servo motor actuators for tilt control applications was studied in [18]. In this section, the advantages of servo motor actuators are highlighted with further features and summarized below:

1. Condition monitoring functions are commercially available in SMDUs, as presented in [29]. ATCS is a safety function. Using the condition monitoring function integrated into the SMDU, premature failure in the servo motor actuator can be detected, and system safety can be increased.
2. Servo motor actuators do not need maintenance and do not exhibit oil leakage problems which can occur in electro-hydraulic (EH) and electro-hydrostatic actuators (EHA) [30–33]. Oil leakage has a negative impact on the safety and performance of electro-hydraulic and electro-hydrostatic actuators.
3. Servo motors can be equipped with electromagnetic brakes. In case of any failure in any component of ATCS, an electromagnetic brake can be applied, and vehicle rollover can be prevented.
4. SMDUs have high torque bandwidth. Therefore, actuator-related delay is not an issue for servo motor actuators. In [34,35], SMDU control loops are studied in detail. Referring to a configuration in [34], the rise time of the position control loop of a servo motor can be 6 ms, and the settling time can be approximately 20 ms. In [35], bandwidth measurements of control loops of an SMDU are given. In [35], the tested bandwidth of the position loop is given as 100 Hz. This yields approximately 3.5 ms rise time for the position control loop of SMDU. These examples show that SMDU and servo motor provides a very fast response.

In [31], the position delay of EHA was analyzed, and a compensation method was proposed. The delay is described as the required time for the pressure to reach the threshold value, which can start the piston cylinder in the EHA system. Besides the above-mentioned advantages, it has been shown in simulations that servo motors can have short regeneration operation and hence reduce energy consumption.

Based on the literature review, it can be stated that this study, together with the authors' previous publication in [18], provides a detailed analysis and design of the DTC system with a servo motor actuator.

The contribution of and organization of this study can be summarized as follows:

- In Section 2: The stability analysis of the DTC method is studied by step response and root locus design tools. It has been shown that the speed control loop of SMDU has contributed to the stability of the tilting system.
- In Section 3: the DTC controller was developed using state feedback control with a pole placement design technique in a previous study by the authors [18]. As a further improvement, the state feedback controller is combined with the disturbance compensation controller [36]. DTC has inherently delayed response [1–4,6–17] because the vehicle driver should apply a steering input at first, and then a lateral acceleration occurs. This phenomenon creates a delay when calculating the tilt control reference by using the system states. On the other hand, when lateral acceleration occurs, and

DTC control reference is applied, tilt actuator torque starts to increase. This is useful feedback to detect the lateral acceleration and cornering request of the vehicle driver. By using the estimated servo motor actual torque and servo motor speed, disturbance compensation is developed. Using SMDU internal signals to design a disturbance compensation is a novel concept in active tilt controller design and adapted from industrial motor control applications [36]. This improvement enables a faster response of the tilt angle, as shown in simulations and experiments.

- In Sections 4 and 5, simulation and experimental results are given, including the power and energy consumption.

2. Analysis and Design of Direct Tilt Controller

2.1. Instability Problem of Three-Wheeled NTV

To analyse the stability problem of NTV, linearization is applied to $\theta = 0$ condition. It is assumed that the tilt angle has small changes. By using the Figure 1, the equation of motion of NTV for tilting is given by Equation (1) [6,7,9]. Friction, damping in the tilting mechanism is not included in (1).

$$(I_x + mh^2)\ddot{\theta} = mgh\sin\theta - ma_yh\cos\theta + T_{tilt} \tag{1}$$

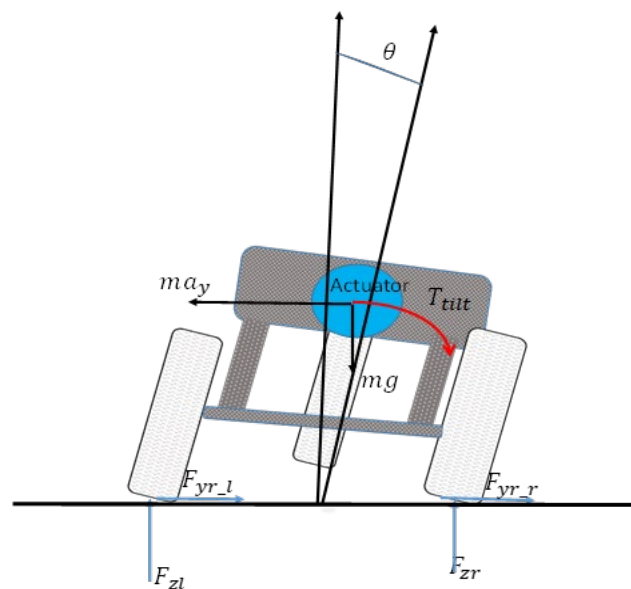


Figure 1. Forces and tilting torque are applied on a three-wheeled NTV during tilting.

Equation (1) is re-arranged as Equation (2) for the open loop transfer function analysis at small tilt angle changes. Lateral acceleration is set to zero for this analysis.

$$(I_x + mh^2)\ddot{\theta} = mgh\theta + T_{tilt} \tag{2}$$

By expressing the time domain expression in (2) into the s-domain, an open loop transfer function without a tilt controller is obtained and given in (3). In (3), tilting torque is the input and tilt angle is the output.

$$TF_{ol} = \frac{\theta}{T_{tilt}} = \frac{1}{(I_x + mh^2)s^2 - mgh} \tag{3}$$

Open loop poles of TF_{ol} is given in (4) as a function of vehicle parameters:

$$p_{ol1,2} = \mp \sqrt{\frac{mgh}{(I_x + mh^2)}} \tag{4}$$

Using the vehicle parameters in this study, open loop poles are calculated as in (5):

$$p_{ol1,2} = \mp 3.05 \quad (5)$$

One of the poles in (4) is on the right side of the root locus curve. Therefore, the tilting system exhibits instability without any controller. Stabilization can be done by different controller types. PD type controller is widely used in the literature [6,7,10]. Section 2.2 describes the stabilization effect of the speed controller of SMDU on the instability problem described by Equations (3)–(5).

2.2. Stability Analysis with Servo Motor Speed and Position Control Loops Servo Motor Control System and Mathematical Model

Field-oriented control of permanent magnet synchronous motor is studied in [37,38]. Mathematical models of control blocks in Figure 2 are given in [37,38]. Referring to Figure 2, the SMDU torque reference is the output of the speed controller. By using a proportional type controller, SMDU torque reference is given by (6) [18]:

$$T_{sm_ref} = \left[(\theta_{smref} - \theta_{sm})K_{pos} - \dot{\theta}_{sm} \right] K_{sp} \quad (6)$$

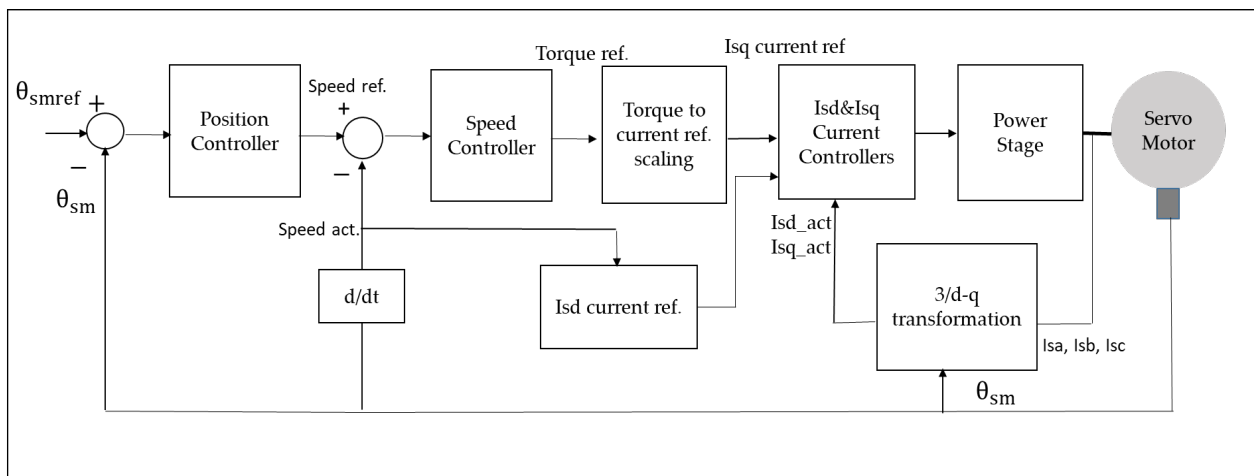


Figure 2. Servo motor control system with inner control loops.

The total inertia reflected on the servo motor shaft is given by (7). The gearbox is coupled to the servo motor shaft to increase the torque at the tilting axis. Therefore, the total inertia reflected at the servo motor shaft is reduced by the inverse square of the gear ratio K_g :

$$I_{sm_tot} = \frac{I_x + mh^2}{K_g^2} + I_{sm} \quad (7)$$

Step response characteristic values of SMDU are set as below. SMDU is set to position control mode:

- Rise time $T_r = 0.25$ s
- Settling time $T_{settling} = 1$ s
- Position overshoot = 0
- Steady-state error < % 3

2.3. Dominant Closed Loop Poles of DTC Type Tilting System

Using the Equations (2) and (6), Equation (8) is obtained and expressed at the servo motor shaft. Transfer function in s-domain is expressed by (9):

Compared to the open loop unstable transfer function in (3), stabilization at the actuator level can be achieved by choosing the proper gear ratio and SMDU control loop gains K_{sp}, K_{pos} [18].

$$\left[(\theta_{smref} - \theta_{sm})K_{pos} - \dot{\theta}_{sm} \right] K_{sp} = \frac{I_{sm_tot}}{K_g^2} \ddot{\theta}_{sm} - \frac{mgh\theta_{sm}}{K_g} \tag{8}$$

$$TF_{cl_sm} = \frac{\theta_{sm}}{\theta_{smref}} = \frac{K_{sp}K_{pos}}{\frac{I_{sm_tot}}{K_g^2} s^2 + K_{sp}s + \left(K_{sp}K_{pos} - \frac{(mgh)}{K_g} \right)} \tag{9}$$

To yield a stable response, the roots of the denominator should be placed at the left half plane of the root locus. Using the second-order equation, the roots of the transfer function in (9) can be calculated analytically as a function of system parameters.

Roots of a second order equation is calculated as given in Equation (10):

$$x_{1,2} = \frac{-b \mp \sqrt{\Delta}}{2a} \tag{10}$$

$$\Delta = b^2 - 4ac \tag{11}$$

Equation (11) is expressed in terms of vehicle and servo system parameters:

$$\Delta = (K_{sp})^2 - 4 \frac{I_{sm_tot}}{K_g^2} \left(K_{sp}K_{pos} - \left(\frac{mgh}{K_g} \right) \right) \tag{12}$$

Considering the stability, the poles given in (10) must be negative to locate the poles at the left side of the root locus. Based on the relationships between (8)–(12), following conclusions are obtained:

- (1) To realize real poles in (10), discriminant in (12) should fulfil the relationships in (13) and (14).

$$\Delta \geq 0 \tag{13}$$

$$(K_{sp})^2 \geq 4 \frac{I_{sm_tot}}{K_g^2} \left(K_{sp}K_{pos} - \left(\frac{mgh}{K_g} \right) \right) \tag{14}$$

The gear ratio, SMDU speed and position controller gains should fulfil the condition in (14).

- (2) SMDU speed control loop contributes to stabilization. It can replace the derivative term used in the PD controller.

$\frac{I_{sm_tot}}{K_g^2}$ is defined by the symbol “a” in the discriminant equation.

By using the high gear ratio, variations in total tilting inertia will have a minor effect on the reflected total inertia on the servo motor shaft. As a conclusion of this, poles $x_{1,2}$ have minor changes. First order damped response is the target characteristic for the position control response of SMDU. Based on the test cases in simulations, the desired rise time is set as 0.25 s and the settling time is 1 s as the target values.

The dominant pole is located at $p_1 = -7.5$. The second pole is very far from the origin and located at $p_2 = -6486$. In this analysis, speed controller gain is set as $K_{sp} = 12$, position controller gain is set as $K_{pos} = 8$.

The schematic in Figure 3 is used to derive the closed loop transfer function in (9). When deriving this transfer function, steering input and lateral acceleration are set to zero.

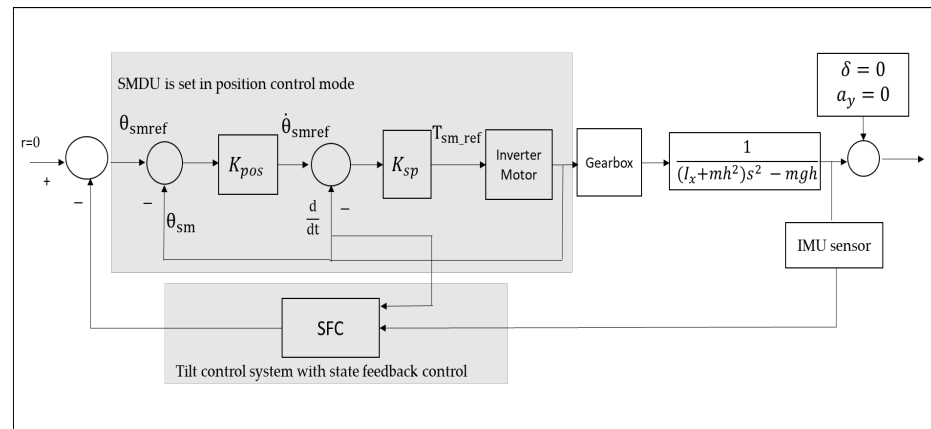


Figure 3. Simplified control schematic for transfer function analysis in Section 2.3.

2.4. State Feedback with Pole Placement Design

Details of controller design with state feedback control are given in the previous study of the authors [18]. In this section, further analysis is given [36]. Maximum longitudinal vehicle speed is set as 10 m/s.

State space equations of tilt control of an NTV is expressed by Equation (15) [15].

$$\dot{X}(t) = AX(t) + Bu(t) \tag{15}$$

The output of the state feedback controller is given as the product of state feedback gain matrix K and system state matrix $X(t)$. The gain for lateral speed is set to zero, as described in [18].

$$\theta_{tilt_ref} = [K_y \ K_{\dot{\psi}} \ K_{\theta} \ K_{\dot{\theta}}] \begin{bmatrix} y \\ \dot{\psi} \\ \theta \\ \dot{\theta} \end{bmatrix} \tag{16}$$

Tilt torque reference is given by (17), which includes the position and speed control loops of the SMDU as proportional controller and gear ratio [18]:

$$T_{tilt} = K_g(K_{sp}K_{pos}K_{\dot{\psi}}\dot{\psi} + K_{sp}K_{pos}(K_{\theta} - 1)\theta + (K_{sp}K_{pos}K_{\dot{\theta}} - K_{sp})\dot{\theta}) \tag{17}$$

$$u = -KX \tag{18}$$

It should be noted that the control input applied to SMDU is the tilt position reference. However, the physical input applied to the servo motor is the torque as a function of the tilt position (angle) reference expressed by the system states in (16).

2.4.1. Root Locus Analysis

By choosing the selected pole locations, the analysis is given below to investigate the steady-state performance of the DTC system at 1 m/s and 10 m/s vehicle speeds [36].

The characteristic equation of a second order system is given by (19) [39–42]:

$$\frac{K_{sys}\omega_n^2}{s^2 + 2\zeta\omega_n s + \omega_n^2} \tag{19}$$

ω_n is the natural frequency and ζ is the damping of the second-order system [39–42].

Pole locations at $V_x = 1$ m/s:

Closed loop poles at 1 m/s are located at: $-2492.9; -190.7; -36.9; -7.9$ as shown in Figure 4.

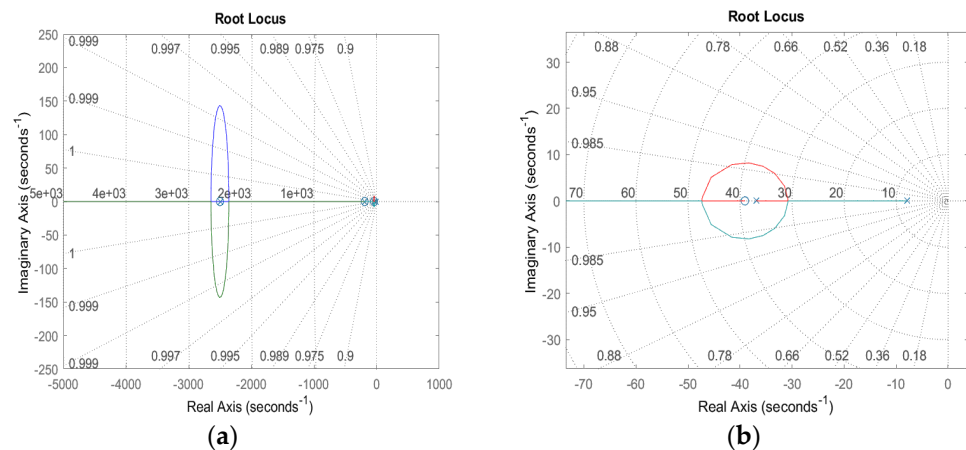


Figure 4. (a) pole locations at $V_x = 1$ m/s (b) Zoomed figure for dominant pole locations at $V_x = 1$ m/s.

The characteristic Equation (19) is given for dominant poles at $-36.9; -7.9$ and expressed in (20).

$$s^2 - 44.8s + 291.51 \tag{20}$$

$\omega_n = 17.07$ rad/s and $\zeta = 1.31$, therefore, the step response is overdamped at $V_x = 1$ m/s.

Pole locations at $V_x = 10$ m/s:

Closed loop poles at 10 m/s are located at $-2342.9; -57.1; -2.8 + 2.4 i; -2.8 - 2.4 i$. as shown in Figure 5.

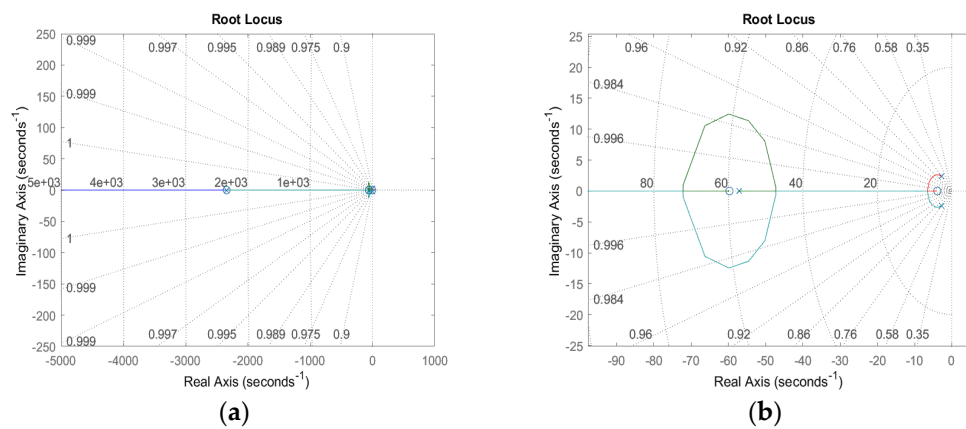


Figure 5. (a) Pole locations at $V_x = 10$ m/s (b) Zoomed figure for dominant pole locations at $V_x = 10$ m/s.

The characteristic Equation (19) is given for the dominant poles at $-2.8 + 2.4 i; -2.8 - 2.4 i$ and expressed in (21):

$$s^2 - 5.6s + 13.6 \tag{21}$$

$\omega_n = 3.68$ rad/s and $\zeta = 0.76$. Damping is less than 1. Therefore, the tilt angle has some overshoot at high speeds.

2.4.2. Step Response Analysis for State Feedback Controller

In Figure 6, step response curves are plotted in Matlab using the state space model in (15) and the transfer function in (9), respectively. Both of the step responses are consistent with each other.

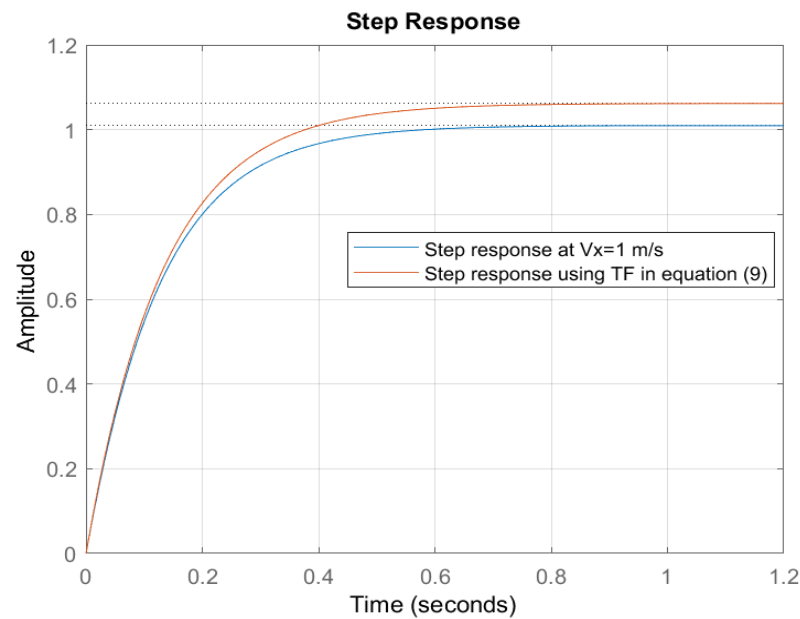


Figure 6. Step response of SMDU in position control mode at $V_x = 1$ m/s using the state space model and step response using the transfer function in Equation (9).

Step response characteristics in Figure 6 are obtained by the `stepinfo()` command in MATLAB and given below:

Stepinfo the using state space model at $V_x = 1$ m/s: RiseTime: 0.2782, SettlingTime: 0.4950, SettlingMax: 1.0094

Stepinfo using the transfer function in Equation (9) RiseTime: 0.2913; SettlingTime: 0.5189; SettlingMax: 1.0620

3. Improvement of DTC: State Feedback combined with Disturbance Compensation

3.1. Industrial Motor Control with Disturbance Torque Compensation

Disturbance compensation is a control concept developed in industrial motor applications [43–47]. The purpose of disturbance compensation is to improve system dynamics against the variations of mechanical load (including mechanical parameters like inertia). In motor control applications, the disturbance compensation term is included at the output of the speed controller. In other words, it is added to the current reference so that the motor torque can rapidly respond to the load variations.

In principle, disturbance compensation is applied through a first-order load observer. The load refers to the mechanical load applied on the servo motor shaft.

In Figure 7, based on the principles given in [43–47], principle control schematic of a disturbance compensation is given for an industrial motor control system.

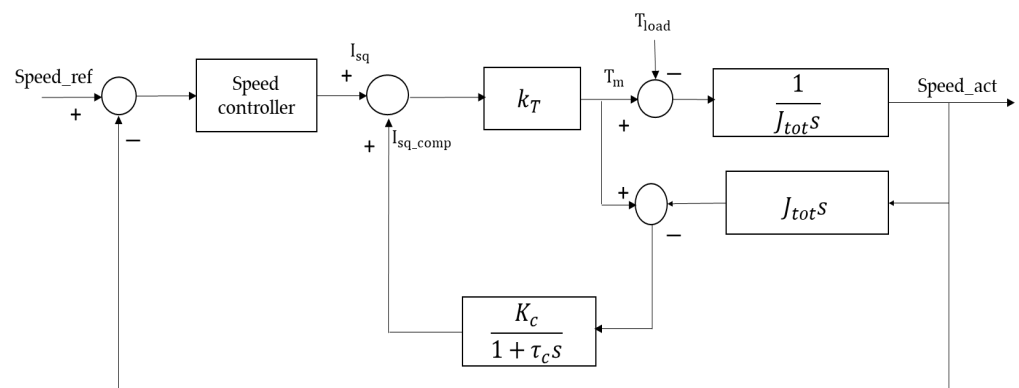


Figure 7. Principle of disturbance torque compensation in industrial motor control.

The equation of motion, including the disturbance torque, is given in Equation (21). Friction and damping factor are not included in (22).

$$I_{sm_tot} \frac{d}{dt} \omega_r + T_L = K_T i_m = T_m \quad (22)$$

T_m is the actual motor shaft torque and is commonly available as a read-out signal in industrial motor controllers (inverters). The use of torque sensors can also be another alternative. However, it will increase the system cost.

K_T is the torque constant of the motor. Load torque (disturbance torque) is given in Equation (23) [43–47]. ω_r is the angular mechanical speed of an electric motor.

$$T_L = T_m - I_{sm_tot} \frac{d}{dt} \omega_r \quad (23)$$

Because of the noise problem of the derivative of speed, authors in [47] proposed using motor speed instead of motor acceleration. Based on this simplification proposed in [47], a simplified model of disturbance observer based on motor speed is given in Equation (24), which includes a gain factor K_c and a time constant τ_c .

$$T_{comp} = \frac{K_c}{1 + \tau_c s} (T_m - I_{sm_tot} \dot{\theta}_{sm}) \quad (24)$$

3.2. Proposed Active Tilt Control with Disturbance Torque Compensation

The principle described in Section 3.1 can be adapted and applied to the DTC-based tilt control system for improved DTC response [36].

Using the linearized tilting motion equation given in [6,9], the mechanical disturbance load applied to the output of the servo motor gearbox is defined by $T_{actuator_distload}$ in Equation (26), which corresponds to the right side of Equation (25).

$$-T_{tilt} + (I_x + mh^2) \ddot{\theta} = mgh\theta - (F_f + F_r)h \quad (25)$$

$$-T_{tilt} + (I_x + mh^2) \ddot{\theta} = -T_{actuator_distload} \quad (26)$$

Actuator load torque (disturbance load) in (26) is applied to a first-order observer as expressed in (27) and (28).

To define the compensation angle, the load applied to the servo motor actuator defined in (26) is multiplied with a first-order transfer function. Equation (27) is the derivative form of compensation angle with notation θ_{compd} . Equation (27) is integrated, and Equation (28) is the compensation angle.

$$\theta_{compd} = -(-T_{tilt} + (I_x + mh^2) \dot{\theta}) \frac{1}{(1 + \tau_c s)} K_c = T_{actuator_distload} \frac{1}{(1 + \tau_c s)} K_c \quad (27)$$

$$\theta_{comp_discsom} = (T_{tilt} - (I_x + mh^2) \dot{\theta}) \frac{1}{s(1 + \tau_c s)} K_c \quad (28)$$

The main contribution of the disturbance compensation is to increase the response of the tilt controller as soon as the estimated actual torque is increased due to the cornering manoeuvre. Principle control schematic of disturbance compensation combined with state feedback is given in Figure 8.

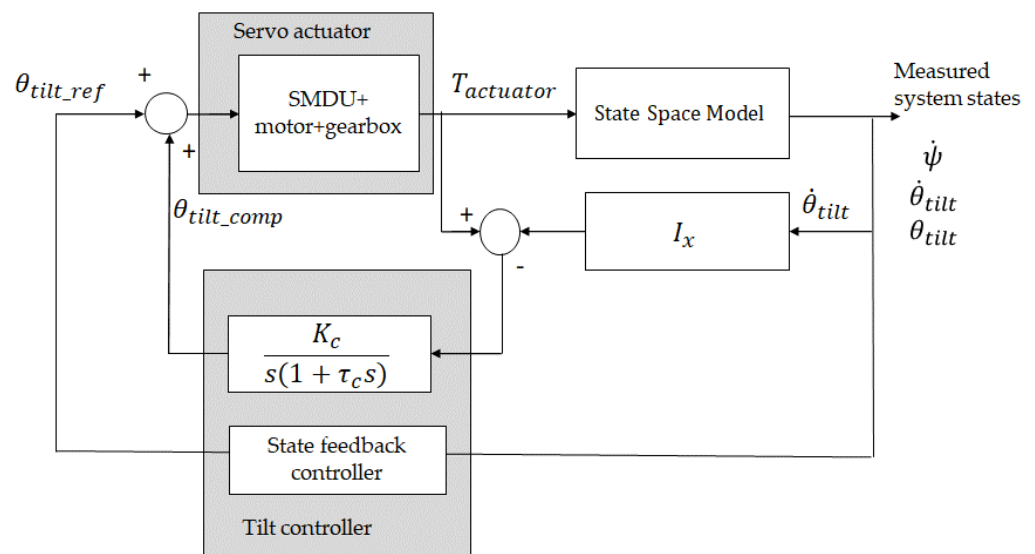


Figure 8. Disturbance compensation in tilt control [36].

Reference Model Control

The reference model control (RFM) concept is introduced in [18]. It is improved further and developed as disturbance compensation [36].

In simulations, the comparison is given between state feedback control (SFC), state feedback combined with disturbance compensation (SFC + DC), and state feedback combined with RFM (SFC + RFM). Principle control schematic of reference model control combined with state feedback is given in Figure 9.

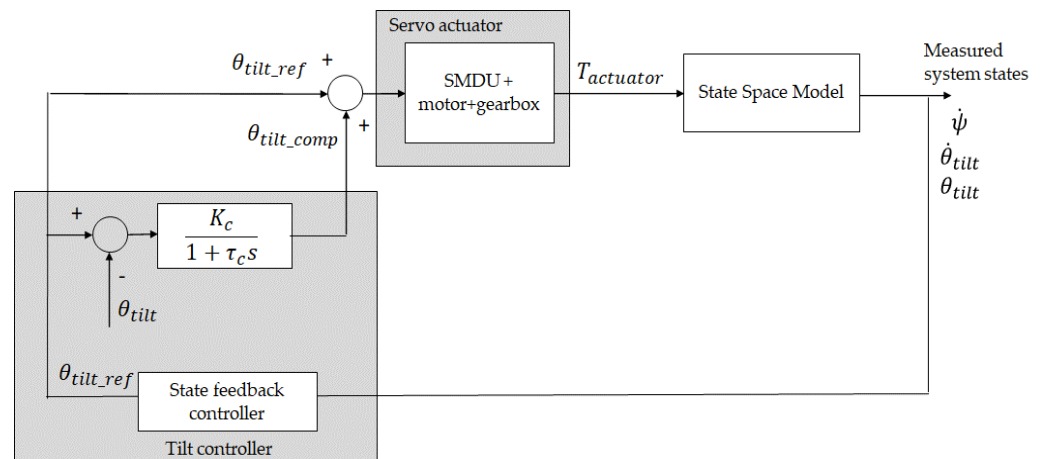


Figure 9. State feedback and reference model control in tilt control [18,36].

The compensation angle with RFM control is defined as:

$$\theta_{tilt_comp_rfm} = \frac{K_c}{1 + \tau_c s} (\theta_{tilt_ref} - \theta_{tilt}) \tag{29}$$

The objective of disturbance compensation and RFM control is to make a compensation effect on the tilt control reference. In this way, the response time of the DTC system can be improved. The compensation angle is applied to the output of the state feedback tilt controller because the state feedback controller outputs the position reference to SMDU.

$$\theta_{\text{tilt_ref_comp}} = \theta_{\text{tilt_ref}} + \theta_{\text{tilt_comp}} \quad (30)$$

Compensation angle $\theta_{\text{tilt_comp}}$ is calculated by either disturbance compensation or RFM control.

4. Simulation

In the Simulink model, the following sub-blocks exist:

- PMSM model with field-oriented control
- State space vehicle model
- State feedback controller
- The compensation angle calculated by the disturbance compensation or reference model control is added to the tilt position reference calculated by the state feedback controller.

The Servo motor is a permanent magnet synchronous motor (PMSM). It has 400 W rated power at 3000 rpm, 1.3 Nm continuous torque, and 3.8 Nm peak torque. This data is used as motor data in the simulation model. The integrated motor inverter is JVL servo motor MAC 402 [48]. The Servo motor shaft is connected to a gearbox with a 330:1 ratio. There are three reasons for using a gearbox with a high gear ratio: (1) Increase the servo motor torque at the gearbox's output. (2) Limitation of the ratio between load inertia to servo motor rotor inertia. This is a critical design parameter studied in motor control applications [49,50]. (3) The Servo motor can be operated at a higher efficiency region on the efficiency map [18]. Controller parameters in simulation are given in Table 2.

Table 2. Controller parameters.

State Feedback Controller	SMDU	DC and RFM
$K_{\psi} = -0.8535 V_x$ $K_{\theta} = 7.6$ $K_{\dot{\theta}} = 0.3$	$K_{pos} = 1.2$ $K_{sp} = 1.2$	$K_c = 0.8$ $\tau_c = 0.02$

It should be noted that signs of state feedback controller gains should be reversed when applying them to Equation (17) to obtain the form in Equation (18), and tilt position reference is multiplied by the gear ratio K_g when applying it to SMDU.

In simulations, it is assumed that the gearbox has 90% efficiency, the SMDU has 96% efficiency, servo motor has 90% efficiency at 10 m/s vehicle speed as an average value. This is an assumption, and the real efficiency of these components can be different at these operating points. Battery energy consumption is calculated by the integral of actuator shaft power and dividing it by system efficiency. It is time average value for the given tilting period.

4.1. Simulation Results

Simulation results are given at 10 m/s vehicle longitudinal speed, and steering input is applied up to 5 degrees [36] as shown in Figure 10.

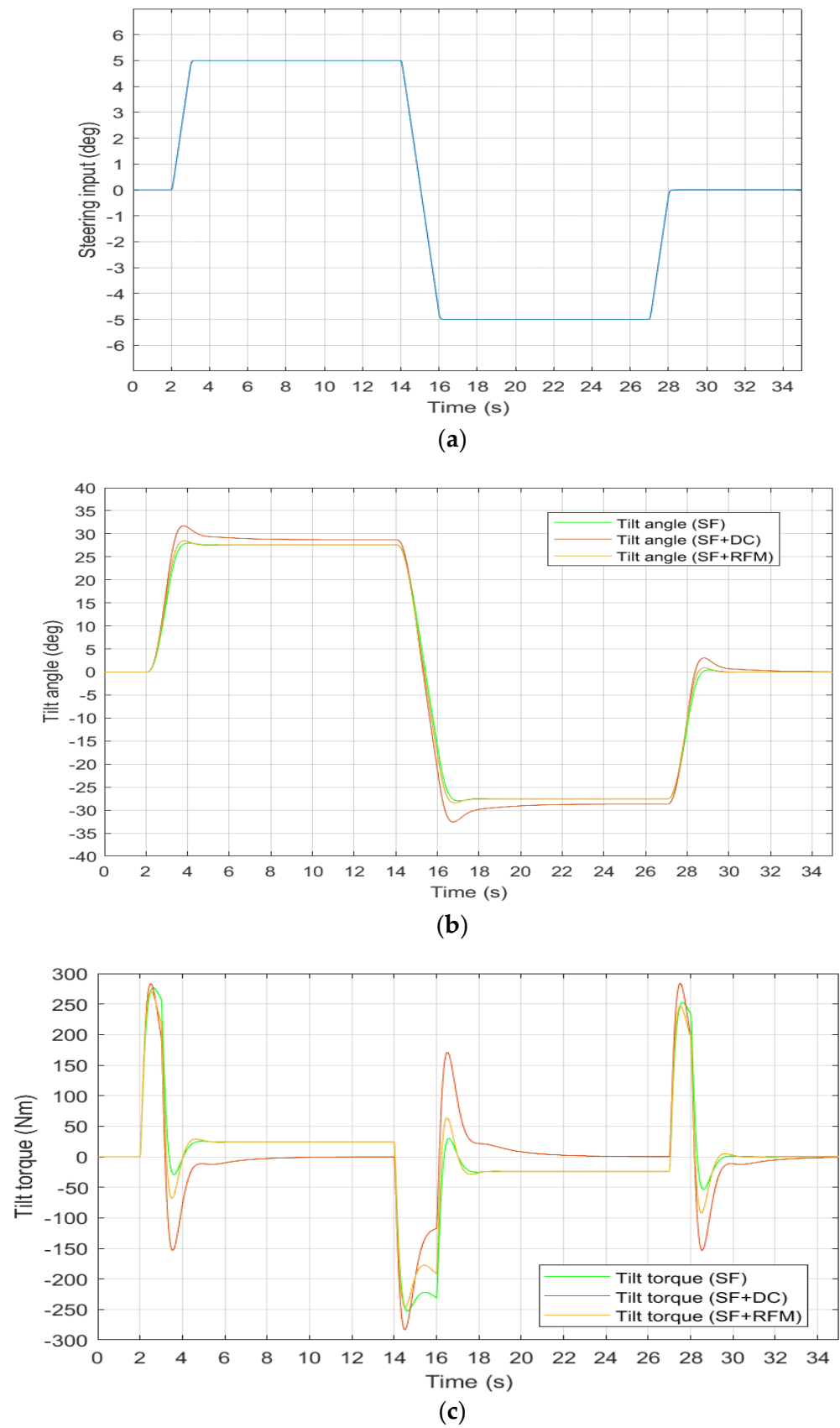
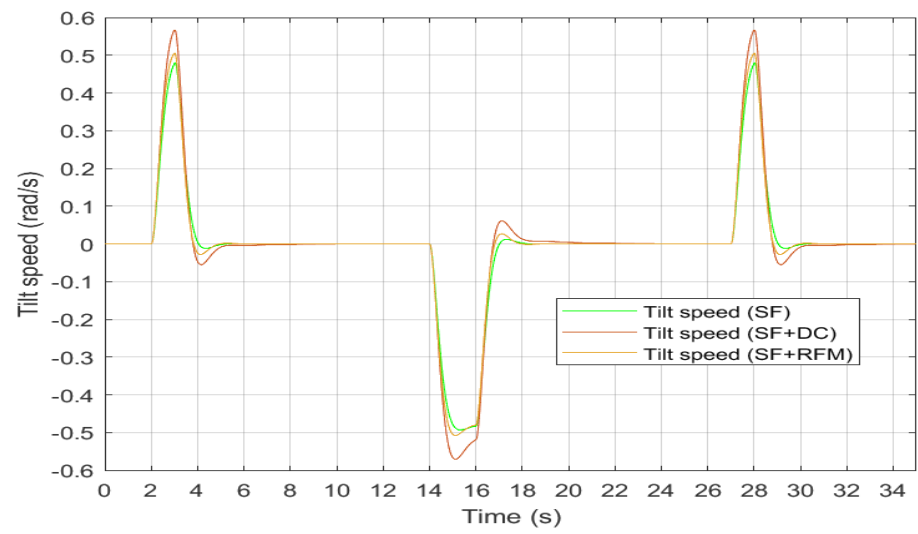
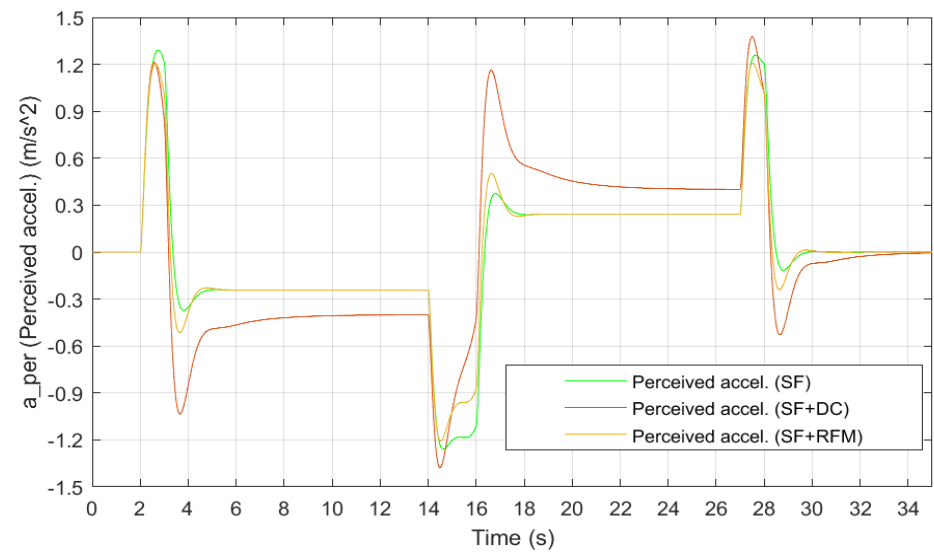


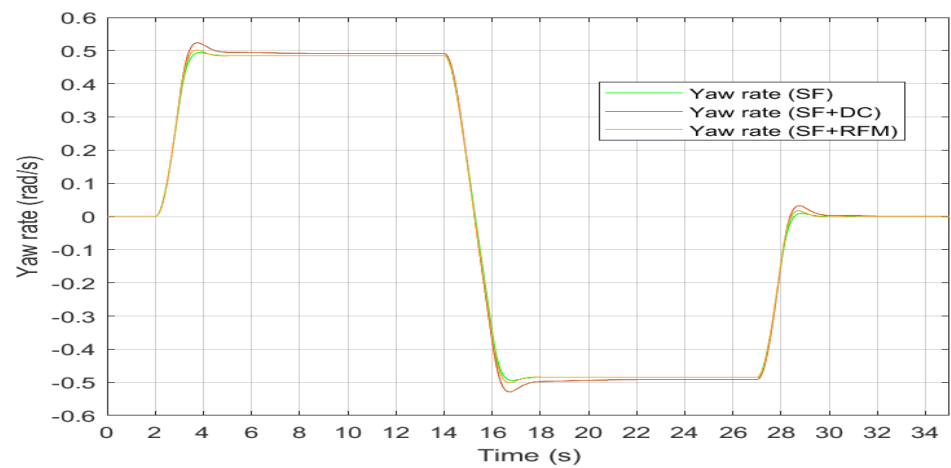
Figure 10. Cont.



(d)

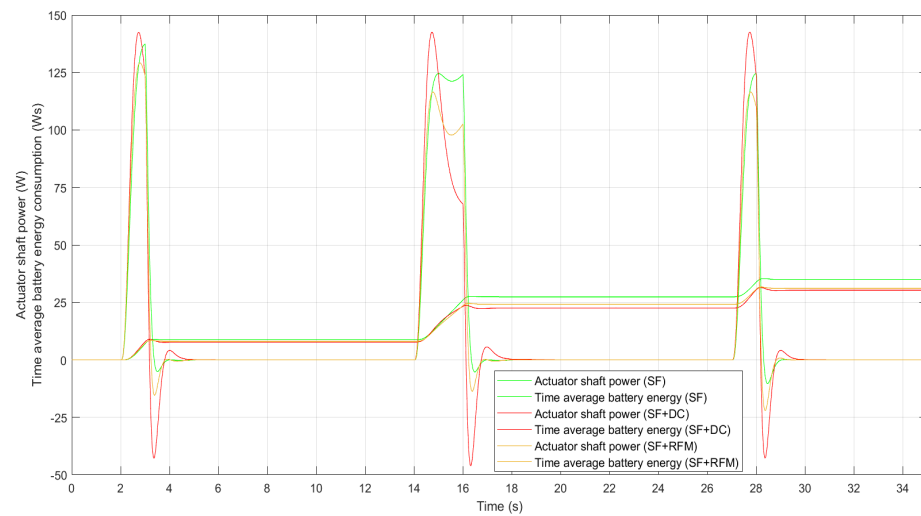


(e)



(f)

Figure 10. Cont.



(g)

Figure 10. Simulation results at 10 m/s and 5 deg. steering input: (a) steering angle (deg.); (b) tilt angle (deg); (c) actuator torque (Nm); (d) Tilting speed (rad/s); (e) perceived acceleration (m/s^2); (f) yaw rate (rad/s); (g) actuator shaft power (W) and battery energy consumption (Ws).

4.2. Analysis of the Simulation Results

4.2.1. Analysis of the Tilt Angle Response

As known in motorcycle driving, stabilization of the vehicle at high speed is more difficult than low-speed driving. The proposed control methods have provided stable operations at up to 10 m/s vehicle speed.

The purpose of the proposed compensation method is to start the tilting as soon as the driver applies the steering input. The response time difference between the three methods in Figure 10b is compared as shown in Figure 11. The peak level and peak time of state feedback is the reference point for the comparison. SF + DC combination reaches 0.70 s earlier to the peak level of SF. SF + RFM reaches 0.40 s earlier to the peak level of SF. This analysis shows that SF + DC combination enables faster tilting than SF and SF + RFM.

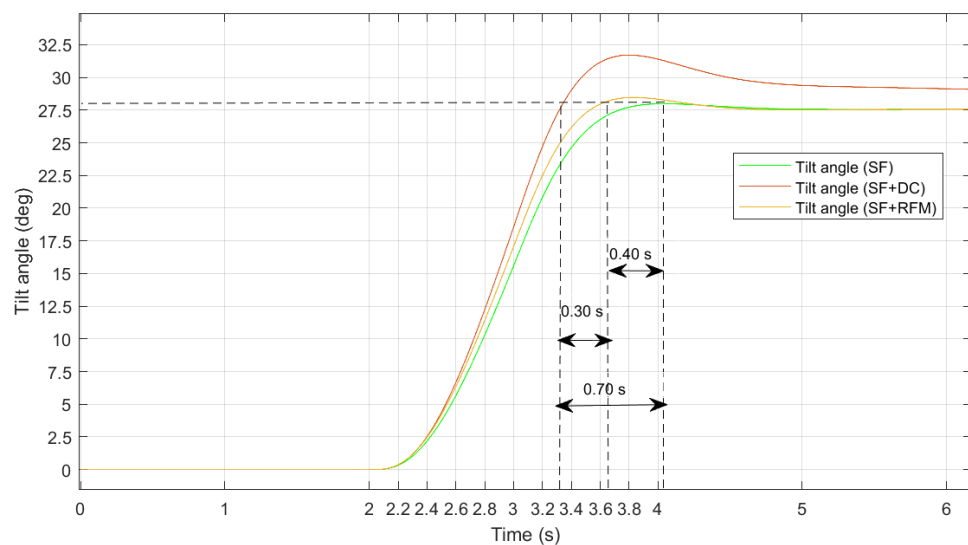


Figure 11. Comparison of response time of tilt angle for SF, SF + RFM and SF + DC.

Tilt angle, tilting torque applied by the actuator, tilting speed (speed of tilt rotation), perceived acceleration and yaw rate shown in Figure 10b–f, respectively, have alignment with the steering input shown in Figure 10a.

4.2.2. Power, Energy Consumption and Regeneration Effect

Regarding the energy consumption, battery energy consumption is 30.36 Ws with SF + DC control, and 35 Ws with SF control.

Fast response provided by state feedback has undershoot effect on the tilting torque. Short-term regenerative operation has been observed in the given simulations. During regeneration, servo motor power changes its sign from positive (motoring mode) into negative direction (generating mode). SF + DC combination has more regeneration effect than SF control.

As shown in simulations, tilting torque has overshoot at initial tilting and undershoot just before settling to the desired tilt angle. When the actuator torque has undershoot, servo motor torque and speed can be in opposite directions during the tilting. During regeneration, the actuator shaft power is at the negative region.

During the tilting manoeuvre, tilting inertia is accelerated and decelerated just before settling to the tilt angle reference. This is shown in Figure 10b,d. During the deceleration moment, the regenerative operation occurs. However, lateral acceleration and gravitational forces act on the tilting inertia in opposite directions. Therefore, regeneration duration is shorter than in industrial servo motor applications with inertial loads.

Even if the regeneration duration is short such as less than 1 s, successive operations in regenerative mode have a cumulative contribution to energy recovery. This property of servo motor actuators has a big advantage over hydraulic actuators and has not been analysed in the state of the art.

In electrical motor drive systems, inertial loads have a regeneration effect on the electrical motor when decelerating [51,52]. Kinetic energy stored in the inertia of the mechanical load is fed back to the motor drive system (inverter). Recovered regeneration energy depends on the total system losses such as friction, motor efficiency map, and inverter efficiency.

$$E_{inertia} = \frac{1}{2} J \omega_r^2 \quad (31)$$

$$E_{tilt_inertia} = \frac{1}{2} I_x \dot{\theta}^2 \quad (32)$$

Kinetic energy stored in inertia is expressed in (31) for electric drive systems [51,52] and expressed in (32) with notations of the DTC system. Deceleration period should also be considered for (31) or (32).

Mechanical losses in the tilting system can be optimized to recover the regeneration energy during tilting.

5. Experimental Results

5.1. Experimental Setup

The tilt controller is implemented on Ecotron VCU 2274A. It is a vehicle control unit used for application software development in electric vehicles as a system controller [53]. Control models developed in Simulink can be embedded into Ecotron VCU (vehicle control unit) using its code generation toolchain. VCU is the system control unit in electric vehicles, and Ecotron VCU enables model-based software development in MATLAB-Simulink [53,54].

VCU runs the tilt control software for the duration of the whole test. SMDU transmits the estimated motor torque signal via the Profinet interface.

Experimental results were performed using the components and prototype three-wheeled electric vehicle shown in Figures 12 and 13. (The figures of the DTC system components in Figures 12a and 13 are sourced from and available in [48,53,55–58]).

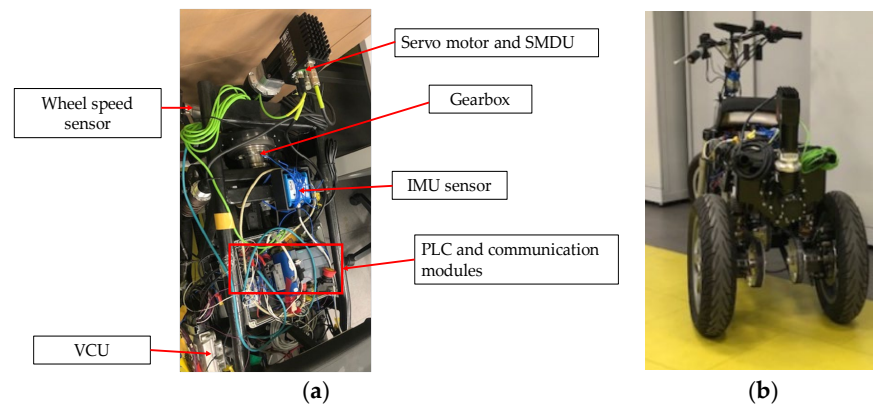


Figure 12. (a) Components of the tilt control system; (b) Experimental 3-wheeled electric vehicle.

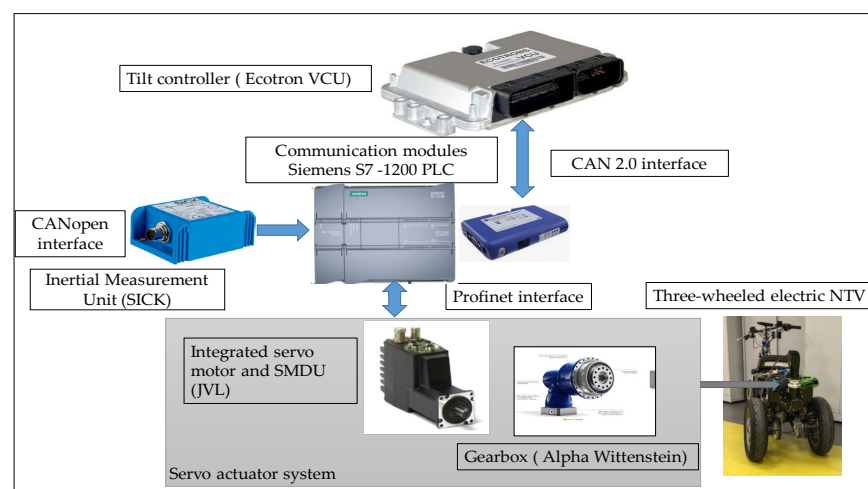


Figure 13. DTC system configuration.

All of the test data in experimental tests were logged in real time by VCU as shown in Figure 13. VCU has a software toolchain for automatic code generation from Simulink models.

There are three test cases which are listed below [36]:

- (1) Standstill step response test
- (2) Cornering test at max. 11 km/h speed. State feedback (SF) and state feedback combined with disturbance compensation (SF + DC).
- (3) Circular trajectory test at max. 6 km/h speed. State feedback (SF) and state feedback combined with disturbance compensation (SF + DC).

Test case 2 was performed at up to 11 km/h speed for the safety of the vehicle driver. The servo motor actuator system is always activated for the test duration. This is required for the safety of the vehicle driver and vehicle as well.

5.2. Step Response Test at Vehicle Standstill

In test case-1, the SMDU reference is set to 6 degrees, and the vehicle is tilted at a standstill condition.

This test corresponds to the experimental verification of the transfer function in Equation (9), which verifies that the speed control loop of SMDU has a stabilization effect. The test duration is 23 s. SMDU position reference is applied stepwise, as shown in Figure 14a. Tilting position from the IMU sensor, servo motor speed, and servo motor estimated actual torque are given as shown in Figure 14. The experimental step response shows that the settling time of the tilting position is approximately 1.5 s, which is consistent with the MATLAB step response with the transfer function shown in Figure 6. Compared

to the MATLAB step response, the experimental step response takes 0.5 s longer. This difference can be described due to the lag caused by the suspension and tire elasticity.

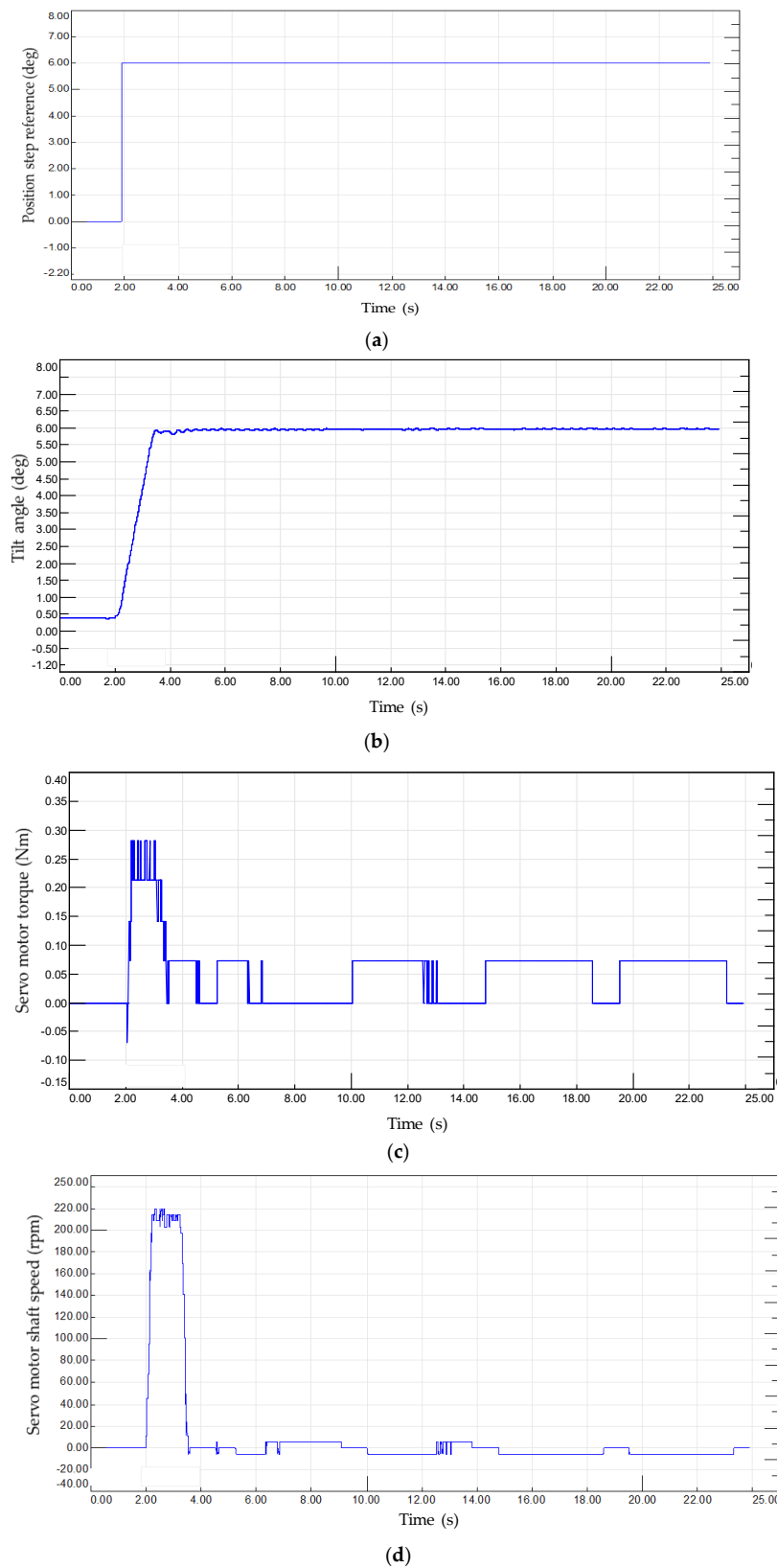


Figure 14. (a) Position reference for SMDU in test case-1 (deg.); (b) Step response of actual tilt angle in test case-1 (deg.); (c) Actual torque of servo motor in test case-1 (Nm); (d) Actual shaft speed of servo motor in test case-1 (rpm).

5.3. Cornering Test at Maximum 11 km/h Vehicle Speed

In the cornering test (test case-2), the vehicle speed is increased up to 3.05 m/s longitudinal speed and stopped as shown in vehicle speed curves. Steering input is applied gradually, approximately up to 14 degrees. The experimental results for state feedback (SF) and state feedback with disturbance compensation control (SF + DC) are given in Figure 15.

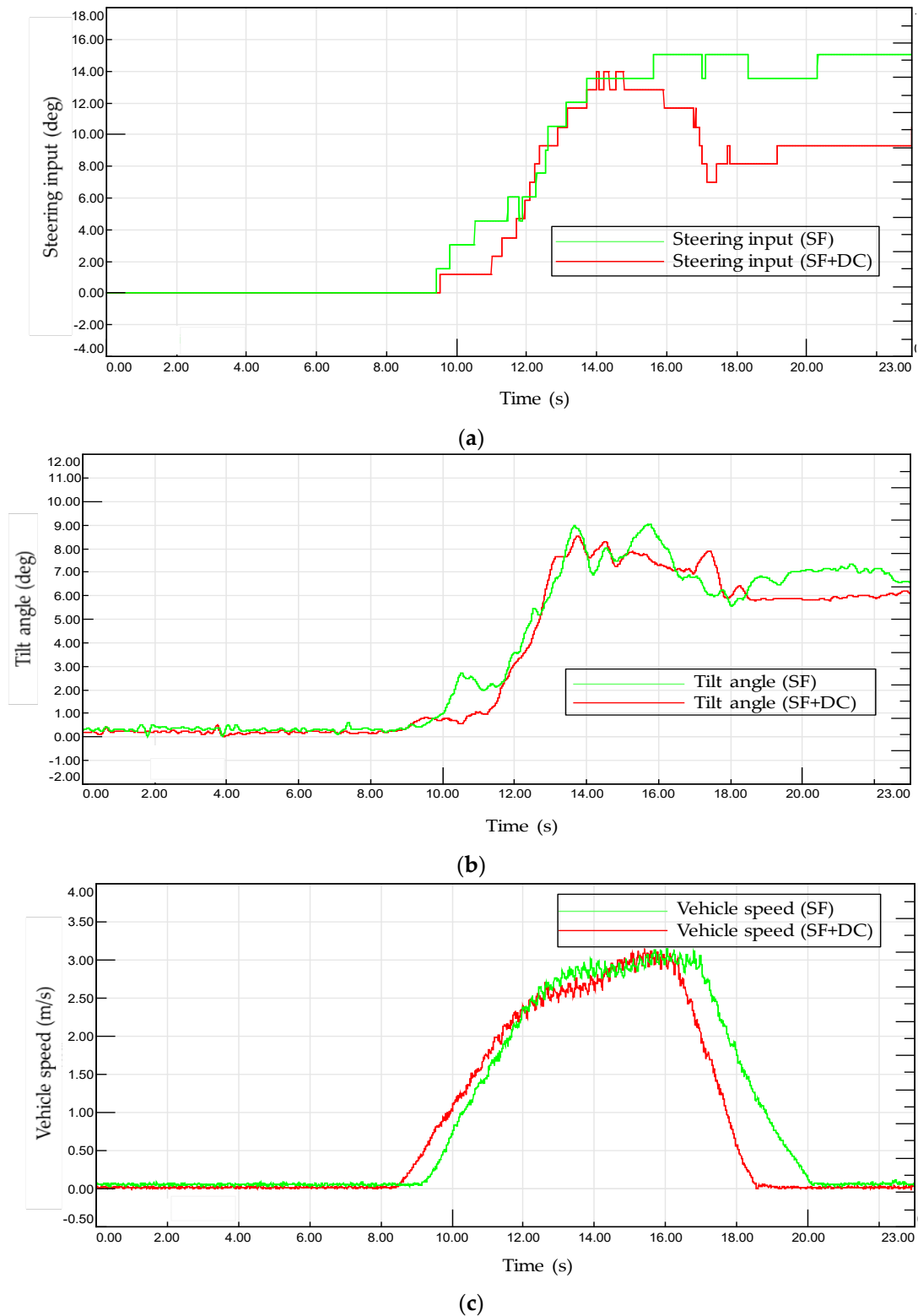
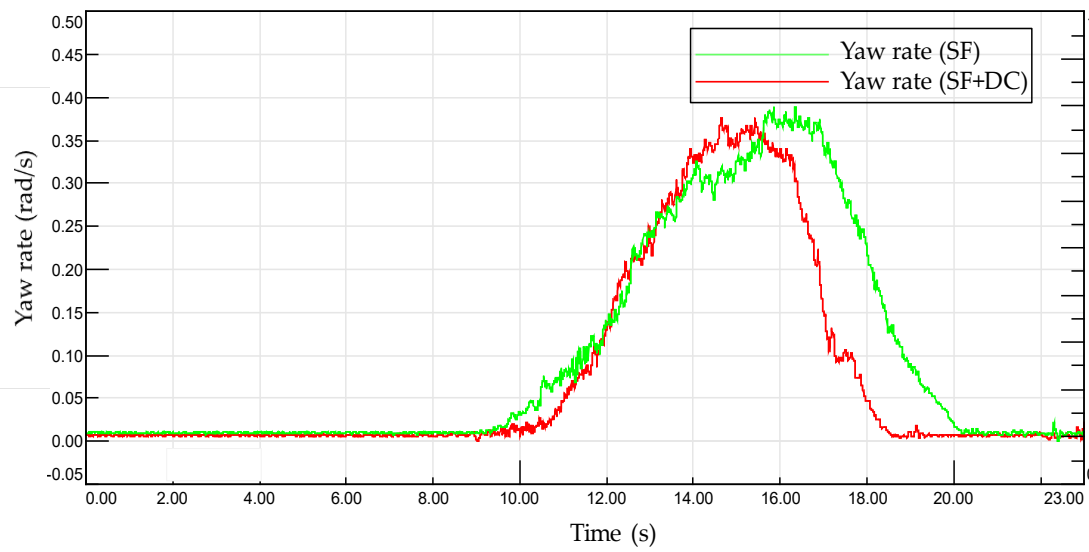
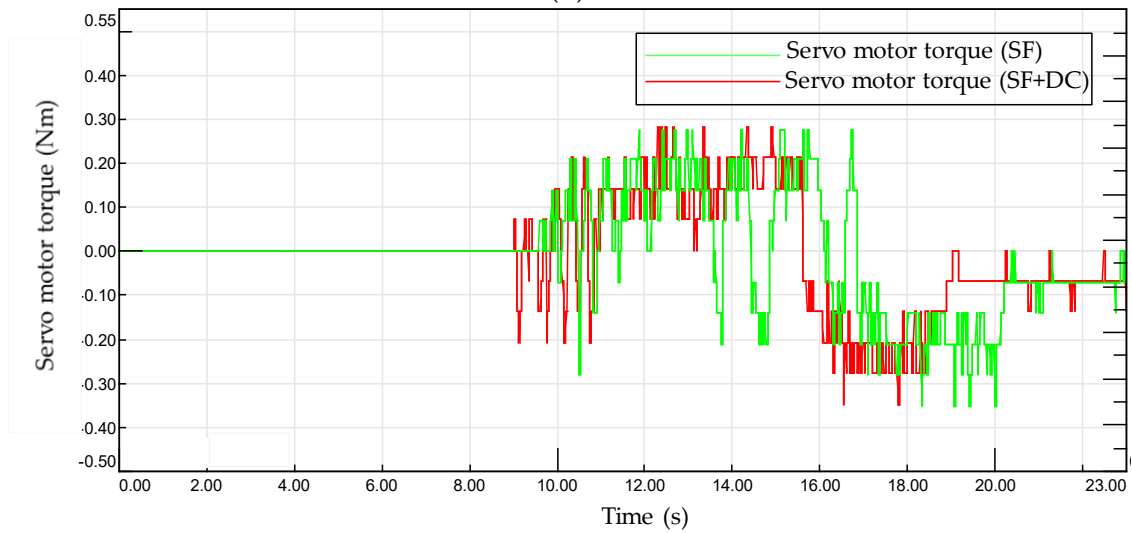


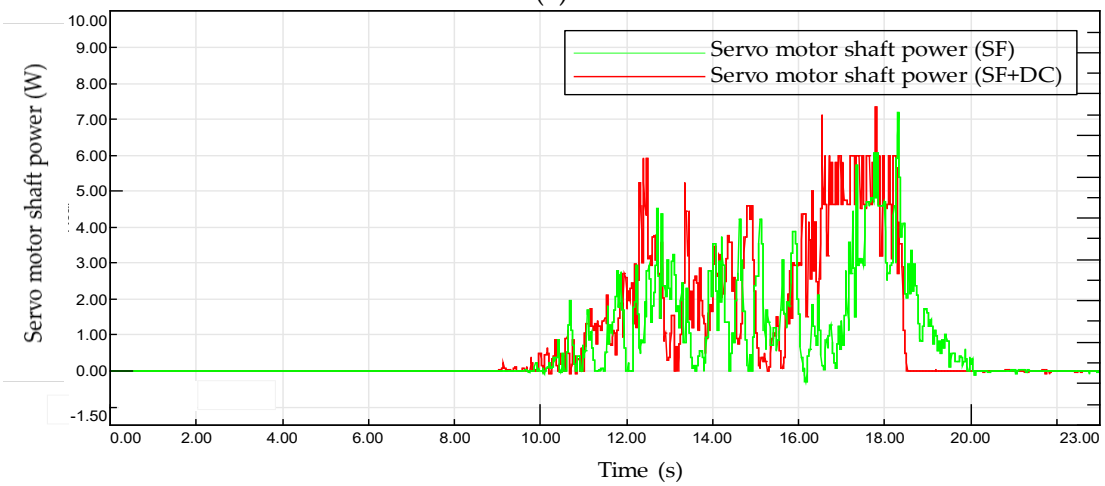
Figure 15. Cont.



(d)

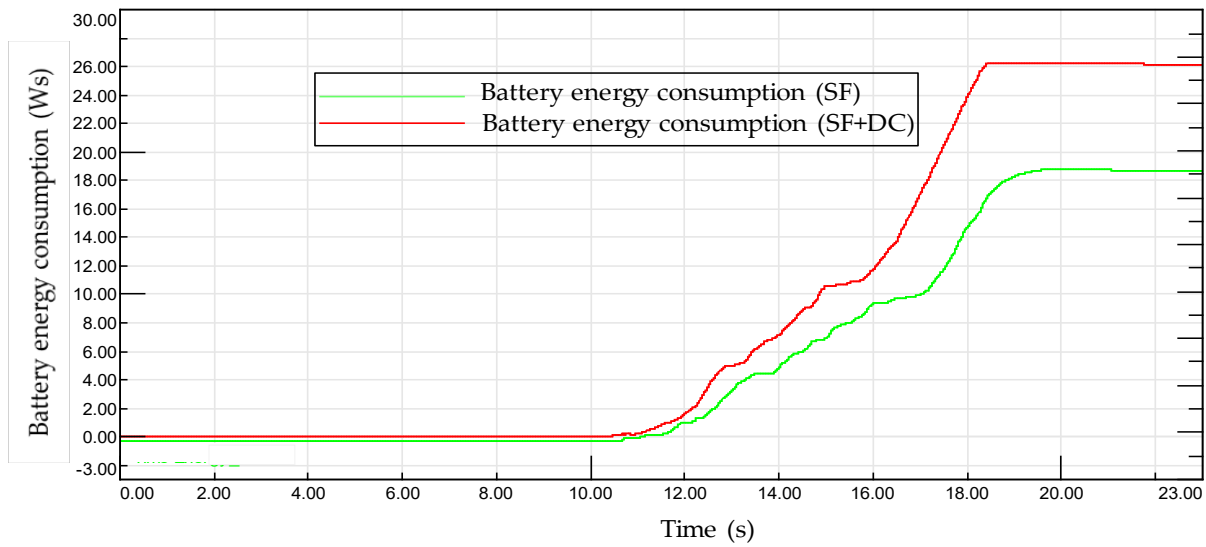


(e)



(f)

Figure 15. Cont.

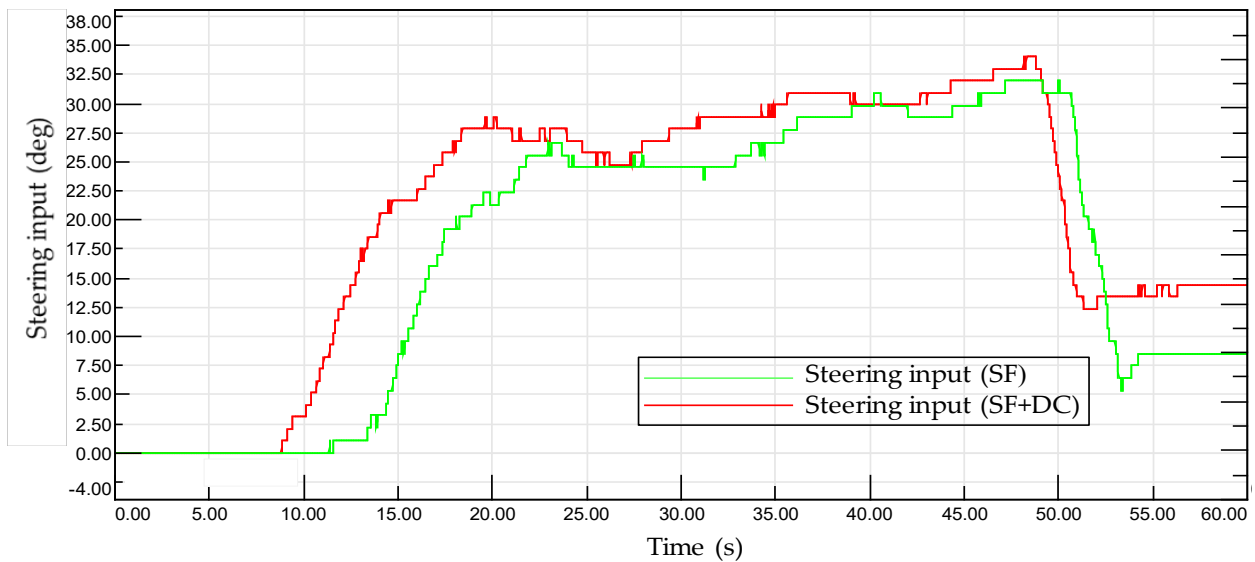


(g)

Figure 15. Cornering test: (a) steering input by the driver (deg.); (b) tilt angle (deg.); (c) vehicle longitudinal speed (m/s); (d) yaw rate (rad/s); (e) Servo motor torque (Nm); (f) Servo motor shaft power (W); (g) Battery energy consumption (Ws).

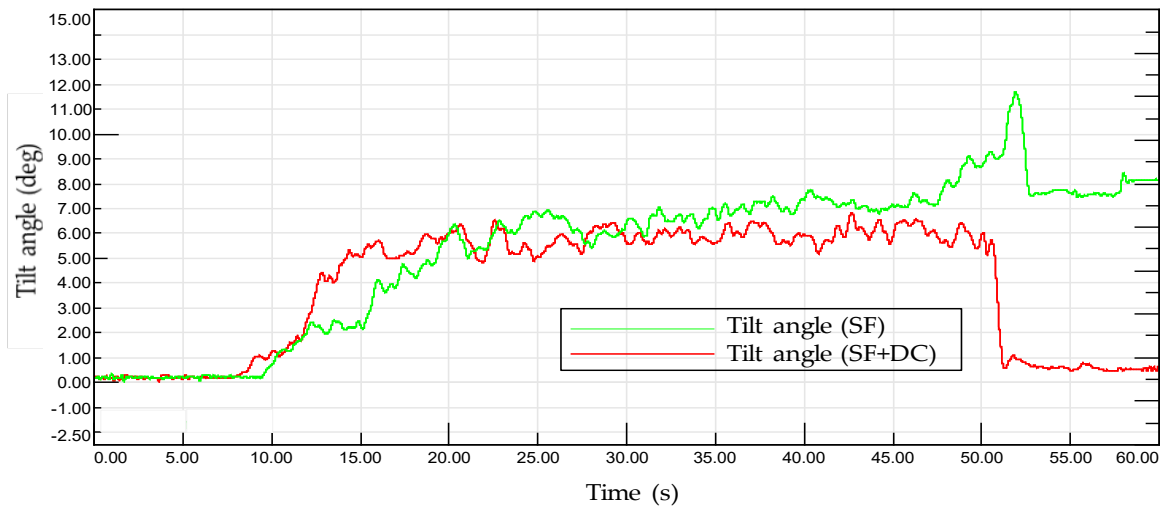
5.4. Circle Trajectory Test at Maximum 6 km/h Vehicle Speed

In test case-3, the vehicle is continuously driven in a circular trajectory with slight variations in steering input and vehicle speed, which changes between 5–6 km/h speed range. Steering input is increased gradually up to approximately 32 degrees in SF and 34 deg in SF + DC control mode. The circle diameter is approximately 4.6 m. The duration of the test is approximately 42 s. The results are given in Figure 16.

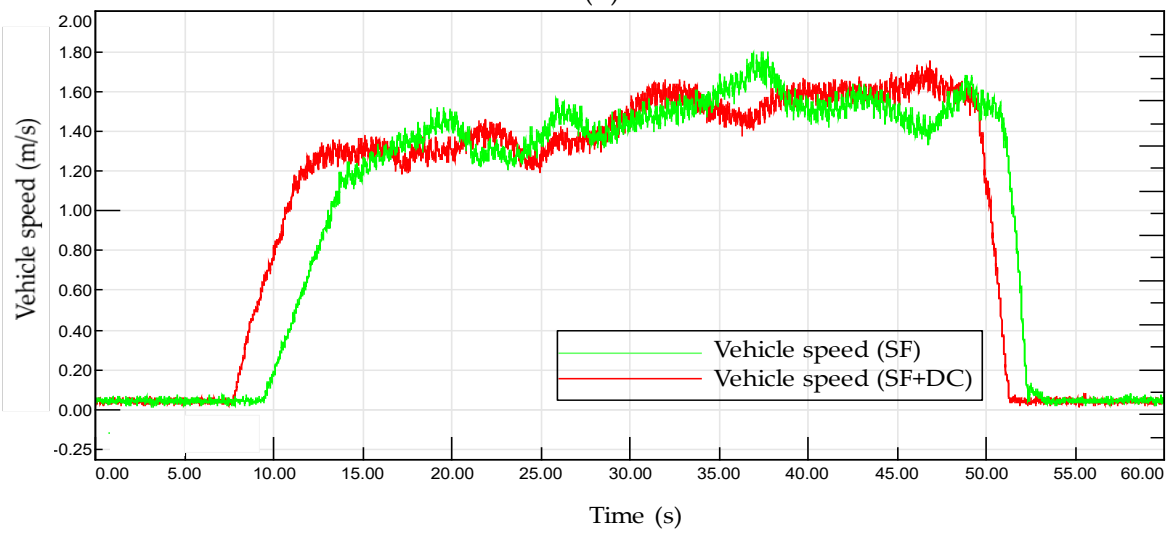


(a)

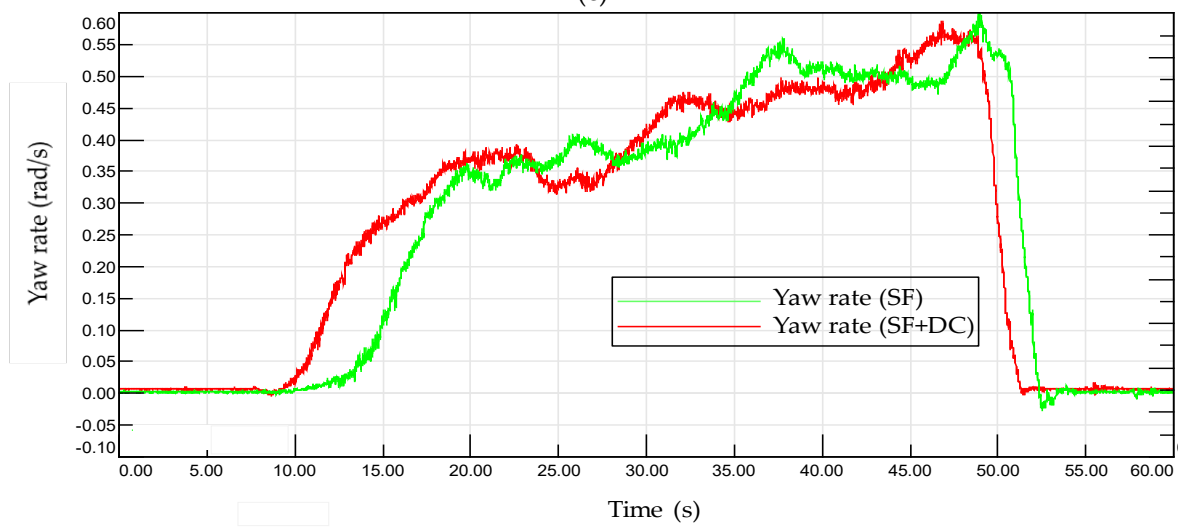
Figure 16. Cont.



(b)



(c)



(d)

Figure 16. Cont.

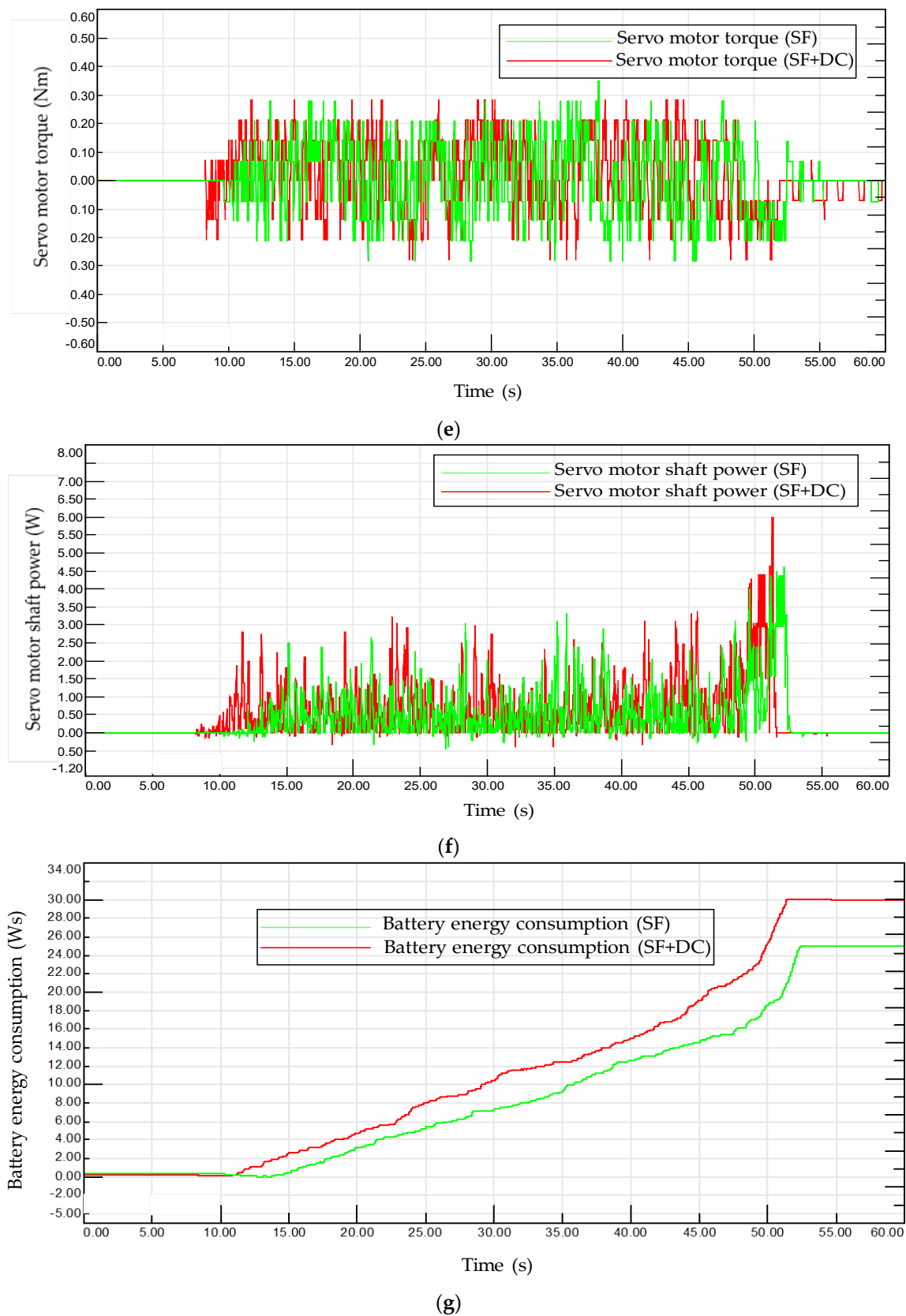


Figure 16. Circular trajectory test: (a) steering input by the driver (deg.); (b) tilt angle (deg.); (c) vehicle longitudinal speed (m/s); (d) yaw rate (rad/s); (e) Servo motor torque (Nm); (f) Servo motor shaft power (W); (g) Battery energy consumption (Ws).

5.5. Analysis of the Experimental Results

To maintain stable operation, it is essential to start the tilting in response to the steering input at the given vehicle speed. The initial start time of the vehicle is different in SF and SF + DC. Vehicle speed and steering input have variations in SF and SF + DC. A comparison between SF and SF + DC can be given concerning the response of the tilt angle.

At the beginning of the tilting period, the SF + DC combination provides a faster response to the steering input. On the other hand, SF has a slightly sluggish response to the steering input and some backwards motion during the initial period of the tilting. In test case-2, at $t = 14$ s, steering input and vehicle speed level are approximately equal for both SF and SF + DC. The tilt angle in SF+DC mode follows a sharper trend up to that point and does not have slight drops as in SF.

In test case-3, at $t = 22$ s, steering input and vehicle speed level are approximately equal for both SF and SF + DC. Up to that point, the rise of the tilt angle has a sharper trend in SF + DC than in SF.

In test cases, 2–3, the efficiency of the SMDU is set as 96%, and the efficiency of the servo motor is set as 80% as the average value for the given test conditions. These efficiency data are only an assumption. Because a detailed efficiency map of the servo motor and SMDU is not available in the datasheets. Servo motor shaft power is calculated as the product of the servo motor's estimated actual torque and speed as read-out data from the Profinet interface of SMDU. Battery energy consumption is calculated by the integral of the servo motor shaft power and divided by the approximated system efficiency.

In test case-2, the peak level of servo motor shaft power is 7.5 W for both SF and SF + DC. Battery energy consumption is 19 Ws for SF and 26 Ws for SF + DC in test case-2.

In test case-3, the peak level of servo motor shaft power is 6 W in SF + DC, and this peak is an instantaneous value at the time of stopping the vehicle. The peak level of servo motor shaft power is 4.5 W in SF in test case 3. Battery energy consumption is 25 Ws in SF in test case-3 and 30 Ws in SF + DC. Differences in total test duration and braking conditions while stopping create minor power and energy consumption differences for SF and SF + DC.

It is shown that servo motor actuator can run as energy efficient tilt actuation system. Both SF and SF + DC combinations run stable at the given test conditions.

6. Conclusions

Proposed control methods have achieved faster response and operation up to 10 m/s vehicle speed for the DTC method in simulations.

Novel and practical methods have been developed in simulation and proven effective and stable in experimental tests.

In experimental tests, the stability of the proposed tilt control methods has been validated for the given test cases. Vehicle tilts successfully in both SF and SF + DC control. SF + DC control is more responsive to the steering input. A disturbance compensation function has been developed using internal signals of SMDU, and performance improvement has also been achieved. This is a cost-effective solution without using any external sensor. An alternative configuration of the disturbance compensation would be using a torque sensor between the servo motor shaft and the gearbox. This configuration can be a future task and enables a comparison of the estimated and the measured actual torque at the servo motor shaft.

In simulations and experimental test cases, servo motor torque is below its continuous torque value of 1.3 Nm. This is a critical result regarding the thermal management of the servo motor because an external cooling system is not suitable for NTV due to the restricted space in the vehicle and extra cost as well.

Future tasks can be listed, such as the fail-safe design of the tilt control system, further investigation of the regeneration capability of the servo motor during various tilting manoeuvres, optimization of the complete system losses, and energy management of the tilt control system, including the vehicle traction and battery systems.

Energy consumption at various vehicle speeds and steering inputs can be uploaded to a database for energy consumption prediction. This will be useful to estimate the required battery energy for the next tilting and possible maximum tilting for a given vehicle speed. This is a critical input for the energy management of the tilt control system.

A fail-safe system can be designed by using the electromechanical brake of the servo motor. In case of any failure in any DTC components, including the SMDU or servo motor, the electromechanical brake can be activated, and vehicle rollover can be prevented. This concept needs further investigation of servo motors with electromechanical brakes and should also be verified by experimental tests.

Author Contributions: Conceptualization, M.K. and O.B.A.; methodology, M.K.; software, M.K.; validation, M.K.; formal analysis, M.K. and O.B.A.; writing—original draft preparation, M.K.; writing—review and editing, M.K. and O.B.A.; supervision, O.B.A. All authors have read and agreed to the published version of the manuscript.

Funding: This research received no external funding.

Institutional Review Board Statement: Not applicable.

Informed Consent Statement: Not applicable.

Data Availability Statement: Not applicable.

Acknowledgments: Authors thanks Ford Otosan A.S. for financial support and for providing the laboratory equipments for the project.

Conflicts of Interest: The authors declare no conflict of interest.

Nomenclature

Θ_{tilt_ref}	Tilt control reference (rad or deg)
m	Total vehicle mass, including driver (290 kg)
V_x	Longitudinal vehicle speed (m/s)
h	Height of center of gravity (0.65 m)
I_x	Tilt moment of inertia (75 kgm ²)
g	Gravity of Earth (9.81 m/s ²)
$\dot{\psi}$	Yaw rate (rad/s)
θ	Actual tilt angle (rad or deg)
$\dot{\theta}$	Actual tilt speed (rad/s)
δ	Driver steering input (rad or deg)
T_{tilt}	Tilt actuator torque (Nm)
θ_{smref}	Position reference of SMDU (rad or deg)
θ_{sm}	Actual position of SMDU (rad or deg)
$\dot{\theta}_{sm_ref}$	Speed reference of SMDU (rad/s or rpm)
$\dot{\theta}_{sm}$	Speed actual value of SMDU (rad/s or rpm)
I_{sm_ref}	SMDU torque reference (Nm)
I_{sm_tot}	Total moment of inertia reflected on servo motor shaft (kgm ²)
I_{sm}	Moment of inertia of servo motor (kgm ²) (0.34 kgcm ²)
K_T	Torque constant of a servo motor (Nm/A)
K_g	The gear ratio of the gearbox (330:1)
K_{pos}	Position controller gain of SMDU
K_{sp}	Speed controller gain of SMDU
$K_{\dot{y}}$	State feedback gain of lateral speed
$K_{\dot{\psi}}$	State feedback gain of yaw rate
K_{θ}	State feedback gain of tilt angle
$K_{\dot{\theta}}$	State feedback gain of tilt speed
K_c	Gain of the reference model and disturbance compensation
τ_c	The time constant of the reference model and disturbance compensation (s)

References

1. Tang, C. Narrow Urban Vehicles with an Integrated Suspension Tilting System: Design, Modeling, and Control. Ph.D. Thesis, University of Waterloo, Waterloo, ON, Canada, 2018.
2. Ataei, M. Reconfigurable Integrated Control for Urban Vehicles with Different Types of Control Actuation. Ph.D. Thesis, University of Waterloo, Waterloo, ON, Canada, 2017.
3. Sindha, J.; Chakraborty, B.; Chakravarty, D. Automatic stability control of three-wheeler vehicles—Recent developments and concerns towards a sustainable technology. *Proc. Inst. Mech. Eng. Part D J. Automob. Eng.* **2017**, *232*, 418–434. [[CrossRef](#)]
4. Docquier, Q. Dynamic Analysis and Control of Narrow Track Vehicles via a Multibody Modeling Approach. Ph.D. Thesis, Ecole Polytechnique de Louvain, Ottignies-Louvain-la-Neuve, Belgium, 2020.
5. Rose, N.A.; Neale, W.T.C. *Motorcycle Accident Reconstruction R-483*; SAE International: Warrendale, PA, USA, 2018.
6. Drew, B.W. Development of Active Tilt Control for a Three-Wheeled Vehicle. Ph.D. Thesis, University of Bath, Bath, UK, 2006.
7. So, S.-G.; Karnopp, D. Active dual mode tilt control for narrow ground vehicles. *Veh. Syst. Dyn.* **1997**, *27*, 19–36. [[CrossRef](#)]
8. So, S.-G.; Karnopp, D. Switching Strategies for Narrow Ground Vehicles with Dual Mode Automatic Tilt Control. *Int. J. Veh. Des.* **1997**, *18*, 518–532.
9. Rajamani, R.; Gohl, J.; Alexander, L.; Starr, P. Dynamics of Narrow Tilting Vehicles. *Math. Comput. Model. Dyn. Syst.* **2003**, *9*, 209–231. [[CrossRef](#)]
10. Kidane, S.; Rajamani, R.; Alexander, L.; Starr, P.J.; Donath, M. Development and Experimental Evaluation of a Tilt Stability Control System for Narrow Commuter Vehicles. *IEEE Trans. Control. Syst. Technol.* **2009**, *18*, 1266–1279. [[CrossRef](#)]
11. Cabrera, L.D.S. Active Tilt and Steer Control for a Narrow Tilting Vehicle. Ph.D. Thesis, Politecnico di Torino, Lambert Academic Publishing, Torino, Italy, 2012.
12. Piyabongkarn, D.; Keviczky, T.; Rajamani, R. Active Direct Tilt Control for Stability Enhancement of a Narrow Commuter Vehicle. *Int. J. Automot. Technol.* **2004**, *5*, 77–88.
13. Gohl, J.; Rajamani, R.; Alexander, L.; Starr, P. Active Roll Mode Control Implementation on a Narrow Tilting Vehicle. *Veh. Syst. Dyn.* **2004**, *42*, 347–372. [[CrossRef](#)]
14. Gohl, J.; Rajamani, R.; Alexander, L.; Starr, P. The development of tilt-controlled narrow ground vehicles. In Proceedings of the 2002 American Control Conference, Anchorage, AK, USA, 8–10 May 2002.
15. Mourad, L. Contrôle actif de l'accélération latérale perçue d'un véhicule automobile étroit et inclinable. In *Automatique/Robotique*; Ecole des Mines de Nantes: Nantes, France, 2012.
16. Mourad, L.; Claveau, F.; Chevrel, P. Direct and Steering Tilt Robust Control of Narrow Vehicles. *IEEE Trans. Intell. Transp. Syst.* **2014**, *15*, 1206–1215. [[CrossRef](#)]
17. Mourad, L.; Claveau, F.; Chevrel, P. A Lateral Control Strategy for Narrow Tilting Commuter Vehicle Based on the Perceived Lateral Acceleration. In Proceedings of the 18th World Congress the International Federation of Automatic Control, Milano, Italy, 28 August–2 September 2011.
18. Karamuk, M.; Alankus, O.B. Development and Experimental Implementation of Active Tilt Control System Using a Servo Motor Actuator for Narrow Tilting Electric Vehicle. *Energies* **2022**, *15*, 1996. [[CrossRef](#)]
19. Yao, J.; Li, Z.; Wang, M.; Yao, F.; Tang, Z. Automobile active tilt control based on active suspension. *Adv. Mech. Eng.* **2018**, *10*. [[CrossRef](#)]
20. Tang, C.; Ataei, M.; Khajepour, A. A Reconfigurable Integrated Control for Narrow Tilting Vehicles. *IEEE Trans. Veh. Technol.* **2018**, *68*, 234–244. [[CrossRef](#)]
21. Tang, C.; Khajepour, A. Integrated Stability Control for Narrow Tilting Vehicles: An Envelope Approach. *IEEE Trans. Intell. Transp. Syst.* **2021**, *22*, 3158–3166. [[CrossRef](#)]
22. Liang, W.; Ahmad, E.; Khan, M.A.; Youn, I. Integration of Active Tilting Control and Full-Wheel Steering Control System on Vehicle Lateral Performance. *Int. J. Automot. Technol.* **2021**, *22*, 979–992. [[CrossRef](#)]
23. Zheng, Y.; Shyrokau, B.; Keviczky, T.; Al Sakka, M.; Dhaens, M. Curve Tilting with Nonlinear Model Predictive Control for Enhancing Motion Comfort. *IEEE Trans. Control. Syst. Technol.* **2022**, *30*, 1538–1549. [[CrossRef](#)]
24. Gao, R.; Li, H.; Wang, Y.; Xu, S.; Wei, W.; Zhang, X.; Li, N. Yaw Rate Prediction and Tilting Feedforward Synchronous Control of Narrow Tilting Vehicle Based on RNN. *Machines* **2023**, *11*, 370. [[CrossRef](#)]
25. Xu, D.; Han, Y.; Han, X.; Wang, Y.; Wang, G. Narrow Tilting Vehicle Drifting Robust Control. *Machines* **2023**, *11*, 90. [[CrossRef](#)]
26. Lapegna, M.; Balzano, W.; Meyer, N.; Romano, D. Clustering Algorithms on Low-Power and High-Performance Devices for Edge Computing Environments. *Sensors* **2021**, *21*, 5395. [[CrossRef](#)]
27. Wu, H.; Chen, C.; Weng, K. An Energy-Efficient Strategy for Microcontrollers. *Appl. Sci.* **2021**, *11*, 2581. [[CrossRef](#)]
28. Becker, P.H.E.; Arnau, J.M.; Gonzalez, A. Demystifying Power and Performance Bottlenecks in Autonomous Driving Systems. In Proceedings of the 2020 IEEE International Symposium on Workload Characterization (IISWC), Beijing, China, 27–30 October 2020.
29. Available online: <https://www.baumueller.com/en/news/press/releases/2022/> (accessed on 20 July 2023).
30. Firoozian, R. *Servo Motors and Industrial Control Theory*; Springer: Cham, Switzerland, 2009. [[CrossRef](#)]
31. Zhang, J.; Li, L.; Zhang, X.; Zhang, T.; Yuan, Y. Delay Analysis and the Control of Electro-Hydrostatic Actuators. *Appl. Sci.* **2022**, *12*, 3089. [[CrossRef](#)]

32. Koitto, T.; Kauranne, H.; Caloniuss, O.; Minav, T.; Pietola, M. Experimental Study on Fast and Energy-Efficient Direct Driven Hydraulic Actuator Unit. *Energies* **2019**, *12*, 1538. [[CrossRef](#)]
33. Wang, M.; Wang, Y.; Fu, Y.; Yang, R.; Zhao, J.; Fu, J. Experimental Investigation of an Electro-Hydrostatic Actuator Based on the Novel Active Compensation Method. *IEEE Access* **2020**, *8*, 170635–170649. [[CrossRef](#)]
34. Weidauer, J.; Messer, R. *Electrical Drives Principles-Planning-Applications-Solutions*; Publicis Publishing: Erlangen, Germany, 2014.
35. Ho, M.-H.; Lai, Y.-S. Controller Design of Servo Drives for Bandwidth Improvement. In Proceedings of the 2017 IEEE 3rd International Future Energy Electronics Conference and ECCE Asia (IFEEEC 2017—ECCE Asia), Kaohsiung, Taiwan, 3–7 June 2017.
36. Karamuk, M. Development of Servo Motor Actuated Active Tilt Control System with State Feedback and Disturbance Compensation Control for A Narrow Tilting Electric Vehicle. Ph.D. Thesis, Istanbul Okan University, Istanbul, Turkey, 2022.
37. Vas, P. *Sensorless Vector and Direct Torque Control*; Oxford University Press: Oxford, UK, 1998.
38. Ong, C.-M. *Dynamic Simulation of Electric Machinery*; Prentice Hall: Hoboken, NJ, USA, 1998.
39. Ogata, K. *Modern Control Engineering*; Prentice Hall: Hoboken, NJ, USA, 2010.
40. Dorf, R.C.; Bishop, R.H. *Modern Control Systems*, 11th ed.; Prentice Hall: Hoboken, NJ, USA, 2008.
41. Franklin, G.F.; Powell, D.J.; Emami-Naeini, A. *Feedback Control of Dynamic Systems*, 7th ed.; Prentice Hall: Hoboken, NJ, USA, 2014.
42. Haidekker, M.A. *Linear Feedback Controls: The Essentials*, 2nd ed.; Elsevier: Amsterdam, The Netherlands, 2020.
43. Senjyu, T.; Kamifurutono, H.; Uezato, K. Robust speed control of DC servo motor based on Lyapunov's direct method. In Proceedings of the 1994 Power Electronics Specialist Conference—PESC'94, Taipei, Taiwan, 20–25 June 1994.
44. Lee, S.-H.; Lee, J.-H.; Huh, U.Y. Adaptive Servo Controller Design Using a Disturbance Observer. In Proceedings of the 1996 IEEE IECON, 22nd International Conference on Industrial Electronics, Control, and Instrumentation, Taipei, Taiwan, 9 August 1996.
45. Hongjuan, Z.; Long, Q. Permanent Magnet Synchronous Motor Servo System with Adaptive Observer. In Proceedings of the International Conference on Computer, Mechatronics, Control and Electronic Engineering (CMCE), Changchun, China, 24–26 August 2010.
46. Wang, G.; Yu, Y.; Yang, R.; Chen, W.; Xu, D.A. Robust Speed Controller for Speed Sensorless Field-Oriented Controlled Induction Motor Drives. In Proceedings of the IEEE Vehicle Power and Propulsion Conference (VPPC), Harbin, China, 3–5 September 2008.
47. Mizuochi, M.; Tsuji, T.; Ohnishi, K. Improvement of Disturbance Suppression Based on Disturbance Observer. In Proceedings of the 9th IEEE International Workshop on Advanced Motion Control, Istanbul, Turkey, 27–29 March 2006.
48. Available online: www.jvl.dk (accessed on 20 July 2023).
49. Vukosavic, S.N.; Stojic, M.R. Suppression of torsional oscillations in a high-performance speed servo drive. *IEEE Trans. Ind. Electron.* **1998**, *45*, 108–117. [[CrossRef](#)]
50. Moscrop, J.; Cook, C.; Moll, P. Control of Servo Systems in the Presence of Motor-Load Inertia Mismatch. IECON'01. In Proceedings of the 27th Annual Conference of the IEEE Industrial Electronics Society, Denver, CO, USA, 29 November–2 December 2001.
51. Lee, J. Inertia Impact on Propulsion and Regenerative Braking for Electric Motor Driven Vehicles. Master's Thesis, Virginia Polytechnic Institute and State University, Blacksburg, VA, USA, 2005.
52. ABB Drives Technical Guide No. 8, Electrical Braking. Available online: https://library.e.abb.com/public/20be376000f34dd6b9c513580cf56423/Technical_guide_No_8_3AFE64362534_RevC.pdf (accessed on 20 July 2023).
53. Available online: <https://www.ecotrons.com/vcu-2/> (accessed on 20 July 2023).
54. Karamuk, M. Review of Electric Vehicle Powertrain Technologies with OEM Perspective. In Proceedings of the 2019 International Aegean Conference on Electrical Machines and Power Electronics (ACEMP) & 2019 International Conference on Optimization of Electrical and Electronic Equipment (OPTIM), Istanbul, Turkey, 27–29 August 2019.
55. Available online: <https://www.sick.com/tr/en/> (accessed on 20 July 2023).
56. Available online: <https://www.hms-networks.com> (accessed on 20 July 2023).
57. Available online: <https://alpha.wittenstein.de> (accessed on 20 July 2023).
58. Available online: <https://www.siemens.com> (accessed on 20 July 2023).

Disclaimer/Publisher's Note: The statements, opinions and data contained in all publications are solely those of the individual author(s) and contributor(s) and not of MDPI and/or the editor(s). MDPI and/or the editor(s) disclaim responsibility for any injury to people or property resulting from any ideas, methods, instructions or products referred to in the content.